A transposon mutation in the *metK* gene promoter suggests that S-adenosyl methionine does not play a role in selenite resistance in *Stenotrophomonas maltophilia* Oak Ridge strain 02

by

FNU Fozia

Submitted in Partial Fulfillment of the Requirements

for the Degree of

Master of Science

in

Biological Sciences

YOUNGSTOWN STATE UNIVERSITY

August 2024

A transposon mutation in the *metK* gene suggests that S-adenosyl methionine does not play a role in selenite resistance in *Stenotrophomonas maltophilia* Oak Ridge strain 02

FNU Fozia

I hereby release this thesis to the public. I understand that this thesis will be made available from the OhioLINK ETD Center and the Maag Library Circulation Desk for public access. I also authorize the University or other individuals to make copies of this thesis as needed for scholarly research.

Signature:

_____

FNU Fozia, Student Date

Approvals:

_____

Dr. Jonathan J. Caguiat, Thesis Advisor Date

_____

Dr. Xiangjia (Jack) Min, Committee Member Date

_____

Dr. David K. Asch, Committee Member Date

_____

Dr. Salvatore A. Sanders, Dean of Graduate Studies Date

ABSTRACT

Stenotrophomonas maltophilia OR02 is a multiple-metal-resistant strain isolated from a metal-contaminated site in Oak Ridge, TN, which grows in the presence of 10 mM of sodium selenite. It appears to form a red-colored precipitate of elemental selenium and gaseous methyl selenide with the characteristic 'garlic' smell. Transposon mutagenesis created a selenite-sensitive mutant, AX55, with an insertion in the putative promoter for *metK*, a gene that encodes an enzyme involved in the synthesis of S-adenosyl methionine (SAM). Thus, SAM could serve as a methyl donor for the methylation of selenide to yield methyl selenide. An experiment on the liquid culture showed AX55 with a MIC (Minimum Inhibitory Concentration) of 10 millimolar selenite, compared with the wild-type strain *S. maltophilia* 02 MIC of 30 millimolar selenite. Growth curves on the wildtype and mutant strains were performed in the presence and absence of 10 mM selenite to further define the mutant phenotype of AX55. In the absence of selenite, both strains grew with an expected lag, exponential, and stationary phase. When 10 mM selenite was introduced during the early exponential phase, the wild-type strain entered a stationary phase. The mutant also entered a stationary phase, but its growth appeared to be more inhibited. An inability of the mutant AX55 to methylate selenide due to the lack of SAM may curtail the growth of the mutant in the presence of selenite. The effect of the mutation on *metK* expression was investigated by extracting RNA from each strain grown both with and without selenite and converted to cDNA using reverse transcriptase. Then, it was PCR-amplified using *metK*-specific primers. Surprisingly, PCR products were obtained for both the wild-type strain and the mutant, and the result suggests that S-adenosylmethionine is not responsible for selenite methylation of selenide. However, some limitations might affect the finding.

ACKNOWLEDGMENTS

First of all, I thank God for all. My sincere gratitude to Dr. Jonathan J. Caguiat for the opportunity to join his research group. Indeed, the abilities that I have gained during this tenure will be crucial in seeking success for all my remaining life. My interest in genetics and microbiology has grown because of this research experience, and I'm motivated to further my horizons as I pursue a PhD. For this, I will always be appreciative.

I am truly grateful to Dr. Xiangjia (Jack) Min and Dr. David K. Asch for agreeing to be on my committee and for their essential advice during my graduate studies. My sincere gratitude is extended to Dr. Michael Butcher, whose supervision during my master's program gave me the information and abilities I have used ever since.

I also want to express my gratitude to my family, friends, the YSU Graduate College, and the Department of Chemical and Biological Sciences for giving me the chance to pursue my higher education overseas. We are grateful for your help and for making this amazing journey possible.

Table of Contents

List of Figures

List of Tables

CHAPTER 1: INTRODUCTION

1.1 Y-12 plant

In the latter six decades of the 20th century, the Y-12 plant at Oak Ridge, Tennessee, played an important role in the national defense of the United States. During World War II, the plant was used for the preparation of uranium intended for the first atomic bomb. In the 1950s, as the Cold War got underway, the Y-12 plant began purifying lithium using mercury to make hydrogen bombs (1). During this operation, about 920,000 kg of mercury were leaked into East Fork Poplar Creek (Poplar Creek) and the surrounding area (2). Four S-3 ponds near the origin of Poplar Creek were used to dispose of acidic wastes contaminated with uranium and other heavy metals (3). These ponds were built without a covering or lining to enable the liquid wastes to evaporate or become decontaminated as they moved through the soil. Unfortunately, most of the waste just seeped into the creek and the ground. These ponds were no longer used in 1983, and the liquid waste was drained and treated. Then, the ponds were filled and covered.

1.2 *Stenotrophomonas maltophilia*

Isolated from Poplar Creek, *Stenotrophomonas maltophilia* Oak Ridge Strain *OR02*, hereinafter indicated as *S. maltophilia 02*, demonstrates resistance to various metal salts like copper, platinum, mercury, gold, cadmium, lead, chromium, and selenium through its capability to convert them into insoluble precipitates. (4). In nature, *Stenotrophomonas maltophilia* is primarily linked to plants however, it is a widespread bacterium that may be found in various environmental settings, including harsh ones. It plays roles in the sulfur cycle, nitrogen cycle, and can also establish itself in hospitals, clean rooms, space shuttles, and other artificial environments (5).

Stenotrophomonas maltophilia is a gram-negative and non-fermented bacillus, that does not ferment glucose or lactose. *Stenotrophomonas maltophilia* in nature is mainly associated with plants, though it is a ubiquitous bacterium able to be isolated from different environmental habitats even extreme ones. These have been known to participate in the sulfur cycle, nitrogen cycle, and the degradation of complicated chemicals (6). With a high morbidity and mortality rate in severely immunocompromised and debilitated persons, *S. maltophilia* is also a global opportunistic human pathogen. Although it often does not infect healthy hosts, it does infect individuals with respiratory system disorders such as cystic fibrosis infection (7). *S. maltophilia* is the sole species within the *Stenotrophomonas* genus capable of infecting humans. It predominantly targets hospitalized and immunocompromised individuals, with a particular impact on ICU patients who have undergone procedures involving prosthetic devices such as feeding tubes, catheters, and mechanical ventilators. This is due to its ability to form biofilms on these surfaces. (8). However, *S. maltophilia* rarely causes community-acquired infections (9). Next to *Pseudomonas aeruginosa*, *Acinetobacter* spp., and the *Burkholderia cepacia* complex, *S. maltophilia* has been regarded as one of the most isolated bacteria in clinical laboratories. (10).

1.3 Microbial Interactions with Metals

Heavy metals are persistent in the environment because they are found naturally in the earth's crust. Processes such as weathering, geothermal activity, forest fires, and microbiological activity can release heavy metals. However, through human activity, this process has rapidly accelerated and increased heavy metals dispersion across the world, posing a serious threat to the environment and human health (11,12). In relation, there has been a clear record of a strong relationship between the rise of highly developed civilizations and the prevalence of heavy metal contamination throughout human history. (12).

Microbes can protect themselves from the harmful effects of metals by developing complex systems of resistance and adaptation. Several overview perspectives on this large and important subject have already been explained at the genetic level (13, 14, 15, 16, and 17). Generally, mechanisms safeguarding the homeostasis of heavy metals might be grouped into four major categories: enzymatic detoxification redox reaction, (dealkylation, sequestration), energy-driven efflux, involving cross-family members of ATPase, RND, and CDF, and reduction of metal uptake. The transport proteins acting for these purposes are of the RND (Resistance-NodulationCell Division) and CDF (Cation Diffusion Facilitator) families. It is also widely known that there exist other non-specific pathways that increase intracellular bacterial resistance to heavy metals.

For instance, bacteria are shielded from harmful heavy metals by the creation of biofilms (18,19). To capture heavy metals, lower their bioavailability, and lessen stress, bacteria also secrete extracellular polymers or siderophores (18, 20).

The growth of numerous sectors, including bioremediation of metal-contaminated settings (21, 22, 23), and bio-mining of minerals from ores or industrial effluents (24), has been made easier by investigations of metal resistance mechanisms. Based on the microorganisms, metal ions, and external environment, there might be direct or indirect interactions between bacteria and heavy metals. Numerous factors influence the ease and speed with which bacteria can metabolize heavy metals, including temperature, pH, food supplies, and metal ions. Due to bacteria's small size and fast growth, bacteria represent the potential to grow in very different environments. This has made them quite useful for environmental cleanup, especially in removing hazardous metals. The bacterial cell wall's functional groups, such as phosphate, sulfate, amino, and carboxyl, are usually where heavy metals bind (25). The three-dimensional arrangement of cells inside biofilms and the

bacterial adherence to the substrate, which differ significantly amongst microbes, have a significant impact on the biofilm-mediated bioremediation effectiveness (26).

Different bacteria are capable of absorbing 1 to 500 mg/g of heavy metals. More importantly, *Pseudomonas aeruginosa* in its Hg-resistant strain uptakes mercury ions with a maximum capacity of about 180 mg/g. Cysteine-rich proteins with a high concentration of sulfhydryl groups are likely to attract mercury ions due to cysteine's increased affinity for the ions. Pb(II) has been observed to accumulate in wastewater by cultures of *Bacillus* and *Pseudomonas*. Cr(VI) can be adsorbed and transformed into Cr(III) by both living and dead *Arthrobacter viscosus*. In the environment, *Staphylococcus epidermis* biofilms effectively remove Cr(VI). *Rhodobacter capsulatus* has a maximal absorption capacity of around 164 mg/g for Zn(II), which is by the Redlich-Peterson and Langmuir isotherms. Cd(II) can be absorbed by *Bacillus cereus* strains at rates of about 32 mg/g for dead cells and 24 mg/g for active cells, respectively. Bacteria are protected from harm by extracellular polymeric substances (EPS), which block the entry of harmful heavy metals. By using the EPS, heavy metal ions such as Hg, Cd, Co, and Cu can accumulate. After adsorption in the bacterial cell, heavy metals can undergo ionic state conversion to decrease their toxicity. Mercuryresistant strains of *Pseudomonas putida* can absorb all mercury from the marine environment and transform it from hazardous Hg(II) to Hg(0), resulting in the reduction of Hg poisoning (25).

Bacteria that can withstand high concentrations of heavy metals have developed to live in hydrothermal vents, mineral deposit areas, and active volcanoes. Bacteria can reduce a broad variety of heavy metal ions. Biological components evolved defenses against heavy metal ions because of their adaptation. Many factors, including the entry of metal ions into the cell, efflux,

sequestration both intracellularly and extracellularly, and redox processes, can affect bacterial tolerance to metals. The extracellular barrier may prevent metal ions from entering the body. Yet, bacteria can take in metal ions through ionizable groups present in their cell wall or capsule. Active transport and efflux systems are used by bacteria to export metal ions from cells. Subsequently, metals accumulate via cellular components (periplasmic proteins, outer membrane proteins) in the periplasm or the outer membrane, or they interact with other chemicals in the cytoplasm. Certain bacteria can use metals and metalloids as donors or acceptors of electrons to produce energy. During anaerobic respiration, bacteria use oxidized metals as terminal electron acceptors. This process also converts hazardous heavy metals to less hazardous forms through enzymatic reduction (27).

The technology of bioremediation is gaining popularity because of its favorable environmental effects, enhanced proficiency, and cost-effectiveness. Several environmentally benign microbial methods are used in bioremediation to lessen environmental contamination. An emerging method of cleaning up pollution is called bioremediation, and it looks to be an effective alternative to costly cleaning equipment. One benefit of bioremediation is that the remediation can be completed onsite, saving on transportation expenses. Additionally, the mineralization or detoxification of contaminants into carbon dioxide, water, and biomass is aided by bioremediation. There are two categories for bioremediation: in situ and ex-situ. Microorganisms that are either aerobic, anaerobic or even both can participate in bioremediation (28).

1.4 Microbial Interactions with Selenium

Selenium (Se) is a metalloid element that is required in trace levels by a wide range of organisms, including mammals and bacteria (29). Selenium, however, has a very small safety margin. In actuality, the range of acceptable levels of this element in various organisms, from lowest (i.e., toxicity) to maximum (i.e., deficiency), is frequently a matter of parts per million or even less (30). Consequently, selenium poisoning poses a serious risk to human health as well as that of livestock and wildlife. Thus, there is a genuine health risk associated with selenium exposure for animals and humans alike. However, in addition to natural sources such as erosion and leaching from seleniferous rocks, other contributors to contamination include the mining of coal, gold, silver, nickel, and phosphate; smelting metals; transport, refinement, and use of oil; burning of fossil fuels in power stations; manufacture of pigments; production of pharmaceuticals; making glass; and frequent irrigation of soils rich in selenium. (31).

Four different oxidation states of selenium are known, which include selenate, Se (VI); selenite, Se(IV); selenide, Se(II); and elemental selenium, Se(0). The toxicities of these types of selenium are solely dependent on how soluble they are in water and, consequently, how bioavailable they are (32). The two soluble forms of selenium, selenite (IV) and selenate (VI) are primarily found in aerobic environments. Oxyanions both tend to bioaccumulate and are harmful (33). While Se (0) is insoluble and so unavailable to biological systems, Se in the form of Se (IV) is more hazardous to most species than Se in the form of Se (VI).

Microorganisms possess the ability to transform different selenium species, by oxidation, reduction, methylation, and demethylation (34,35). During the past 20 years, microbial selenium oxidation has not attracted much interest in these transformations, perhaps because studying lowrate oxidation is more challenging (36). Assimilatory, dissimilatory (37), reduction processes

and biosynthesized nanoparticles (35, 38, 39, 40), bioremediation (41), biogeochemistry, ecophysiology (36), and applications have all been the subject of several outstanding reviews published in recent years (38,42). Most of the research to date has concentrated on a variety of distinct assimilatory and dissimilatory reduction mechanisms, especially in aerobic conditions. It has also addressed the growing applications of selenium reduction and methylation, as well as associated techniques (43).

"Assimilatory reduction" refers to the reduction of selenium for inclusion into seleno-amino acids, whereas "dissimilatory reduction" generally refers to the use of selenium as an anaerobic electron acceptor coupled to respiration and energy generation. Reduction of selenium oxyanions without coupling to energy conservation serves as a mechanism of detoxification. Selenate and selenite can serve as terminal electron acceptors for prokaryotes, which form insoluble, nanostructured Se (0), elemental selenium (44). Under aerobic or microaerophilic conditions, some bacteria and fungi can also achieve the reduction of selenium oxyanions to Se (0) as an element of their detoxification response (45) or in phototrophic bacteria., to maintain redox homeostasis. Microbial oxidation, alkylation/dealkylation, assimilatory, and dissimilatory reduction react with these selenium oxyanions (46).

1.4.1 Selenium transporters

The cysAWTP operon is the sulfate ABC transporter complex., is the mechanism by which *Escherichia coli* absorbs selenium (VI) (47). The identical sulfate transportation pathway that *E. coli* uses for Se (VI) uptake appears to be used by the obligatory aerobic bacteria *Comamonas testosteroni* strain S44 (48). Use of low-affinity phosphate transport system (*ΔpitA* mutant) and high-affinity phosphate transport system (*ΔpstA* mutant) mutants, which were previously studied for tellurite transport, to be carried out for selenite absorption and reduction. (49). The *ΔpitA*

mutant's cultures showed a slower selenite to Se (0) reduction, despite both mutants growing well in the presence of 1 mM selenite. This suggests that the low-affinity phosphate transporter plays a role in selenite uptake is significant in *E. coli*. However, since cytosolic selenite reduction was not entirely inhibited in the *pitA* mutant, *E. coli* has an alternate selenite absorption system or systems (50). In the photosynthetic bacterium Rhodobacter sphaeroides strain IL-106, the polyol transporter is named Smok. for Se(IV). Such a transporter has not been reported in any other bacterium (51).

Several strains of bacteria react with oxyanions differently from one another, especially in terms of how they manage oxyanion uptake, reduction, and overall growth. Growth patterns of different strains are influenced by their distinct oxyanion processing processes and efficiencies. To adapt to shifting environmental conditions and metabolic requirements, bacteria also use a variety of transporters to absorb oxyanions into the cytoplasm. However, various transporters depending on the bacterial growth stage are used by different species. This also includes phosphate and sulfate permease systems because the oxyanions share the charge and trigonal pyramidal shape with these molecules. Another problem is the acetate transporters which would have interactions with oxyanions in case they mimic the mono-carboxylate group. The effect of Se uptake may be based on the limited knowledge concerning the mechanisms of regulation and genomic responses to these oxyanions. (52).

1.4.2 Reduction of selenium oxyanions by assimilatory processes

Reduction of selenium oxyanions is done through assimilatory reduction via two paths: nonspecific and specific. The specific pathway involves the formation of selenocysteine, the 21st amino acid, which is then incorporated into seleno-proteins. On the other hand, the nonspecific pathway involves the assimilation of selenium into Sec and seleno-methionine—Se-Met, the 22nd amino

acid—through the sulfate assimilation pathway. Free Sec can sometimes be directly taken up into selenylated proteins, although it is highly toxic, causing inhibition of growth. (53). Most of the selenium compounds in the diet come from amino acids, selenomethionine, selenocysteine, and selenium methyl-selenocysteine, apart from the anion's selenium and selenite. Hydrogen selenide arises during selenium metabolism via different ways. This compound is a forerunner to selenocysteine and is incorporated into selenoproteins with the help of a Sec-specific tRNA – SectRNA [Ser]Sec. Hydrogen selenide can be methylated to excretory forms like dimethylselenide, trimethylselenonium, and Se-methyl-N-acetylselenohexosamine or phosphorylated to form selenophosphate. Selenite may undergo direct reduction to selenide by glutaredoxin or glutathionylate to seleno-/di-glutathione. SelMet is metabolized via the same pathway as Met, the transsulfuration pathway, which leads eventually to the conversion of methionine to cysteine. Afterwards, selenocysteine β-lyase converts Sec into selenide and alanine. Se-methylselenocysteine undergoes a reaction with SBL to form methylselenol. Besides, glutaminase K and L-amino acid oxidase showed activity transaminating the methylseleno-amino acids Semethylselenocysteine and SelMet into β-methylselenopyruvate and α-keto-γ-methylselenobutyrate. (54)

1.4.3 Reduction of selenium oxyanions by dissimilatory processes

Reduction mechanisms of Se(IV) and Se(VI) vary widely in different species of bacteria. Moreover, in a single bacterium, there are multiple paths for the reduction of Se (IV). SeNPs are usually major products of dissimilatory reduction of both Se (IV) and Se(VI) and could be formed both under anaerobic and aerobic conditions. Several pathways of Se (IV) reduction mechanisms have been described previously, as follows: (i) thiol group-mediated Painter-type reactions; (ii) reduction mediated by the thioredoxin-thioredoxin reductase system; (iii) siderophore-mediated

reduction; (iv) sulfidemediated reduction; and (v) dissimilatory reduction, and other pathways (55–57).

1.5 Use of Selenium as Terminal Electron Acceptors in Bacterial Energy Metabolism

Bacteria using either selenate or selenite, or both, as terminal electron acceptors for respiration in either aerobic or anaerobic conditions are called selenium-respiring bacteria. This group of microorganisms use selenium compounds in their energy metabolism (35). For the couples, SeO_4^{2-}/SeO_3^{2-} and SeO_3^{2-}/Se^0, the reduction potentials under typical circumstances are +0.48 V and +0.21 V, respectively. These potentials are significantly higher than those needed for sulfate reduction (SO_4^{2-}/H_2S), but they are lower than those needed for nitrate reduction (NO_3^-/N_2) (58,59).

Selenate and selenite, two selenium oxyanions, are gradually reduced during bacterial selenium respiration. Elements of selenium (Se^0) with a red color precipitate and selenium nanostructures are the products of this process. Two consecutive reactions carry out the whole biological reduction of selenium from selenium salt to elemental selenium (35, 60)

$$SeO_4^{2-} + 2e^- + 2H^+ \rightarrow SeO_3^{2-} + H_2O \qquad Equation\ 1$$

$$SeO_3^{2-} + 4e^- + 6H^+ \rightarrow Se^0 + 3H_2O \qquad Equation\ 2$$

Selenium nanostructures are produced by the reduction of selenium oxyanions to elemental selenium (Se^0). Metalloproteins, which include cofactors for molybdenum and iron, aid in the process of selenium respiration. The process has been thoroughly investigated and documented in

several bacterial model strains (61). The biogeochemical cycle of selenium depends on selenite respiration, although it has not received as much research attention as selenium respiration from selenate. It was possible to identify and describe a potential respiratory selenite reductase (Srr) by combining biochemical, genetic, and proteomic investigations. This study identifies it as a protein member of the complex iron–sulfur molybdoenzyme family (62).

1.6 Detoxification of selenium oxyanions by bacteria

Reduction mechanisms have a baseline resistance to environmental factors and chemicals in some cases (63). The most common detoxification pathway of selenium or selenite reduction is insoluble Se(0), which subsequently precipitates to form an extracellular or intracellular particle. These particles get deposited into the cytoplasm, membrane, or cell wall, thus contributing to the formation of Se nanostructures (64). Reduction of both takes place under either condition, although in general, this reduction process is faster with selenite than with selenate. Three main ways through which selenate or selenite can be reduced by bacteria are: 1) Through specific or nonspecific enzymes, largely periplasmic or cytosolic oxidoreductases, that work in both conditions; 2) by a Painter-type reaction using thiols; lastly, this takes place via interaction with siderophores like pyridine-2,6-bisthiocarboxylic acid. (65).

1.6.1 Enzymatic detoxification

Selenate and selenite can be reduced to elemental selenium [Se(0)] by a variety of enzymatic systems, including fumarate reductases, and nitrate, sulfite, and nitrite reductases. For example, *T. selenatis* AXT mutants defective in nitrate reductase are unable to reduce nitrite or selenite suggesting the reduction of selenite under anaerobic conditions may involve this enzyme (66). This occurs through interaction with siderophores, such as pyridine-2,6-bisthiocarboxylic acid It has

recently been demonstrated that Rhizobium sullae HCNT1 is capable of reducing millimolar concentrations of selenite by a copper-containing nitrite reductase Nir (67). In Escherichia coli, selenium is reduced to elemental selenium either by the periplasmic nitrate reductase NapA or by the cytoplasmic nitrate reductases NarGHIJ and NarZUWV (63).

1.6.2 Thiol-driven reactions

The reduction of selenite to elemental selenium Se (0) through a reaction involving thiols (68). Painter first demonstrated the synthesis of selenium disulfides in 1941. Also, it makes references to the reaction between selenite and thiol groups. (68).

$$4RSH + H_2SeO_3 \rightarrow RS - Se - SR + RSSR + 3H_2O \qquad Equation\ 3$$

Selenite reacts with GSH, the most abundant thiol in cyanobacteria, proteobacteria, and eukaryotic cells. The reaction generates an intermediary called selenium-di-glutathione, which is a substrate for glutathione reductase with Km and Vmax values equivalent to those for GSH. In this reaction, Se-di-glutathione and NAD(P)H glutathione reductase are converted into the highly unstable selenium persulfide anion, shown in GS-Se– (69).

$$GS - Se - SG + NAD(P)H \rightarrow GSH + GS - Se^- + NAD(P)^+ \qquad Equation\ 4$$

$$GS - Se^- + H^+ \rightarrow Se^0 + GSH \qquad Equation\ 5$$

This altered form of the primary reaction leads to the superoxide anion. Comparison of in vitro chemical reduction of selenite by glutathione with the response to selenite mediated by *E. coli* and *Rhodospirillum rubrum* reaches the same conclusion (70).

$$6GSH + 3SeO_3^{2-} + 4H^+ \rightarrow 3GSSeSG + 2O_2^- + 5H_2O \qquad Equation\ 6$$

Superoxide anions are cleared from biological systems by superoxide dismutase and catalase to avoid oxidative stress, and this could be why two different forms of superoxide dismutase are produced when *E. coli* is grown on selenite (71). Other thiol-containing biomolecules besides glutathione might be involved. For example, the *E. coli* thioredoxin system reduces both selenite and Se-diglutathione. A scheme that has been proposed involves reduction of Se-diglutathione by thioredoxin, is reduced subsequently by NADPH-dependent thioredoxin reductase (72,73).

$$\mathrm{Trx(SH)_2 + GS - Se - SG \rightarrow Trx - S_2 + GSH + GS - Se^- + H^+} \qquad \text{Equation 7}$$

$$\mathrm{Trx - S_2 + NADPH + H^+ \rightarrow Trx(SH)_2 + NADP^+} \qquad \textit{Equation } 8$$

The mechanism of selenite reduction includes three steps. The first step is an enzymatic process where NAD(P)H-dependent reductases, such as glutathione or thioredoxin reductases, generate a labile persulfide anion. Next, the selenite is reduced abiotically to form Se-diglutathione with the concomitant production of reactive oxygen species in a second step. Lastly, Se(0) abiotically forms. Six molecules of GSH restore the original reducing power in this sequence (70).

Several bacterial strains have been isolated owing to their high efficiency of selenite reduction to elemental selenium, Se(0), using thiols in both aerobic and anaerobic conditions (74). One of the best-studied examples is Stenotrophomonas maltophilia SeITE02, which was isolated from the rhizosphere of the Se-hyperaccumulating legume Astragalus bisulcatus grown in seleniferous soil. It has been shown that when S. In the medium, with either glucose or pyruvate as a carbon source in the presence of selenite, the cells of maltophilia SeITE02 produce membrane vesules that surround extracellular nanostructures of Se(0). This already hints at a bacterial implication in the efflux of Se(0) nanostructures out of the cells. (75). Elemental Se occurs in nature in various

allotropic forms, both amorphous and crystalline, including amorphous, a-Se, and crystalline: monoclinic and trigonal. Thus, amorphous Se tends to convert into more stable crystalline forms under the action of heating, various chemical reagents, and other physicochemical processes (76). Several important steps have been suggested to transform amorphous selenium (a-Se) into selenium crystals. First, intracellular synthesis is used to create a-Se nanospheres. These nanospheres are then discharged into the extracellular environment, where they aggregate and finally crystallize. The exact mechanisms underlying the formation, assembly, release, and modification of these comparatively large nanospheres—especially based on their size in proportion to the cell's size—remain unknown. It is thought that many such uncharacterized proteins, enzymes, and transport complexes could play important roles in these reduction cycles. Recently, proteomic studies have implicated a variety of proteins that may be involved in the reduction of Se (IV) (77). Examples include glutathione reductase and the RND (resistancenodulation-division) transport systems, which have already been shown in other bacteria to be components of selenium reduction (78,79).

1.6.3 Siderophore-driven detoxification

The broad-spectrum metal chelator siderophore PDTC contributes to reduction of selenite to elemental selenium Se(0) is a detoxification step in Pseudomonas stutzeri KC. Microorganisms secrete siderophores as part of their iron acquisition system; these are iron-specific chelators, particularly under conditions of low iron availability. The selenite concentration could be reduced by binding to PDTC (pyridine-2,6-dithiocarboxylate) or its hydrolysis product, DPA (dipicolinic acid-pyridine-2,6-bis(carboxylic acid)). Synthesis and excretion of PDTC thus represent a means of environmental detoxification that prevents selenite from entering cells by facilitating its extracellular reduction to metalloids (80).

1.7 Methylation of Selenium

Studies have demonstrated that bacteria control the methylation of selenium by converting selenite (SeO_3^{2-}) and selenate (SeO_4^{2-}) into volatile compounds including dimethyl di-selenide and dimethyl selenide (81,82). Most research shows that when selenium is initially present as an oxyanion, selenium volatilization depends on reduction and methylation processes. So Se(VI) or Se(IV) are first reduced to Se(0) or Se(II) and then methylated to DMSe (41). Given the large number of reactions and intermediates that have been proposed to be involved, including MeSeH, dimethyl disulfide (DMDS), dimethyl selenone, and Se aminoacids (SeMet and SeCys), methylation appears to be the most important or differentiating step (83,84).

Elemental selenium, selenate and selenite, and numerous seleno amino acids were identified sources of DMSe generated by soil *Corynebacterium* resting cell suspensions. From selenite and Se(0), cell-free extracts generated DMSe; where S-adenosylmethionine accelerated the process. Additionally, methionine was converted to DMSe with a garlic-like odor by resting cell suspensions of methionine-utilizing *Pseudomonas* (85). Similar research has been done on the interactions between mixed microbial communities and sulfur compounds in sediments, sewage, soils, and waterways. DMSe, DMDSe, and an unidentified component were produced when sewage sludge was cultured with sodium selenite or Se(0). It was believed that the unknown volatile molecule was dimethyl selenone, or $(CH3)_2SeO_2$. Moreover, this finding seemed to have significant implications because dimethyl selenone was not previously identified as a microbial metabolite. Moreover, it was suggested by Challenger's group that it was the last intermediate before DMSe's created (86).

The enzymes involved in selenium methylation have mostly unknown biochemistry and genetics. An intriguing substitute for the utilization of microorganisms that respire selenium is said to be important bioremediation by the volatilization of selenium from contaminated locations (87). In *S. maltophilia* SeITE02, studies suggested that glutathione and protein reactive thiols played an important role in the reduction of SeO_3^{2-} and in the formation of Se (0) (88). Under conditions where thiol groups of proteins or peptides react with selenite, it is indeed possible to reduce it to elemental selenium. This has been referred to as the "Painter-type" reaction, which has been suggested as a common mechanism for microbial detoxification against oxyanions (18). Selenium methylation consists of both reduction and methylation reactions. It was reported that soil and sewage sludge microorganisms convert inorganic selenium compounds, such as selenite or elemental selenium, to dimethyl diselenide, dimethyl selenide (89), and dimethyl selenone (90). The proposed mechanism of selenium methylation by soil Corynebacterium involves a series of steps: first, the selenite reduction to elemental selenium, this reduction is followed by further transformation into selenide, which is then methylated to produce dimethyl selenide. (91).

It was demonstrated that Zein and L-methionine strongly enhanced selenium volatilization, while DL-homocysteine produced much smaller increases. Selenium volatilization was found to follow a first-order reaction with constant percentage release over time (92). The cloning of the thiopurine methyltransferase gene from *Pseudomonas syringae*, a bacterial enzyme, confers on *E. coli* the ability to volatilize selenite to dimethyl selenide. The enzyme also provides for the conversion of selenomethionine or (methyl)selenocysteine to DMSe and dimethyldiselenide using Sadenosylmethionine as the methyl donor (93). It was shown that the bacterial thiopurine methyltransferase gene from freshwater bacteria is responsible for the methylation of most selenium compounds to DMSe and DMDSe. This was demonstrated for the isolate Hsa.28, most similar to

Pseudomonas anguilliseptica, which produced large amounts of these methylated selenium compounds when cultivated on sodium selenite or (methyl)selenocysteine. Hsa.28 showed strong enhancement of DMSe and DMDSe emission in freshwater, indicating involvement of bTPMT in natural selenium methylation (94). The *mmtA* gene discovered in freshwater bacteria resistant to both selenite and selenate specifies a new class of selenium methyltransferases. Overexpression of *mmtA* in *E. coli* grown with selenium resulted in overproduction of DMSe and DMDSe. These MmtA-like sequences, upon phylogenetic analysis, diverged into two groups: one cluster comprised S- and O-methyltransferases, the other with the UbiE C-methyltransferases, with some neighboring sequences displaying selenium methylation activity as well (95).

1.8 SAM

SAM stands for S-adenosylmethionine and is the major methyl donor for most methylation reactions. It donates the methyl group to cytosine and adenosine bases in DNA, rRNA, and tRNA, and a host of proteins and smaller molecules. Such methylation is crucial for life in any form from the simplest to the highest-order level (96-99). The radical S-adenosylmethionine (AdoMet) superfamily comprises thousands of proteins involved in a wide variety of biochemical processes in every form of life. Their sequences are encoded by the *metK* gene encoding a 384-residue polypeptide. Synthesis of SAM showed that also ATP can act as an adenosine donor. (100). SAM is synthesized by binding the sulfur group of methionine with the fifth carbon of ribose in ATP. The coupling involves the concomitant release of pyrophosphate and inorganic phosphate. Upon donation of the terminal methyl group (101), SAM is converted to S-adenosylhomocysteine. This latter product is degraded into adenine and homocysteine by a cyclic regenerative pathway (96).

CHAPTER II: HYPOTHESIS

The goal is to detect the expression of the *metK* gene in the wild type and mutant in the presence and absence of sodium selenite. The hypothesis is that if S-adenosylmethionine has a role in *metK* gene expression, then transcription of the *metK* gene will be reduced in the mutant AX55 relative to the wild-type *Stenotrophomonas maltophilia 02* in both the presence and absence of sodium selenite.

CHAPTER III: MATERIALS AND METHODS

3.1 Bacterial Strains and Growth Media

Stenotrophomonas maltophilia was obtained from the American Type Culture Collection, Manassas, VA. Competent Escherichia coli EC100D™ pir-116 were purchased from Epicentre, Madison, WI, now an Illumina Company, and their products are distributed by Lucigen, Middleton, WI. Lysogeny Broth (LB) medium was purchased from Fisher Scientific, Waltham, MA. The LB media were made with 10 g/L tryptone, 5 g/L sodium chloride, and 5 g/L yeast extract. To make the LB agar plates, 1.6% agar was added to the LB broth, and it was bought from Amresco, of Solon, OH. Kanamycin was added to the LB media at a concentration of 800 µg/mL, which would maintain the transposon insert in the AX55 mutant from Amresco, Solon, OH.

3.2 Genomic Preparations

DNA from both the Gram-negative bacterial cells of *Stenotrophomonas maltophilia* 02 (wild type) and the mutant AX55 was isolated using a Promega DNA purification kit (Promega's Wizard kit). Cells were first lysed in 600 µl nuclei lysis solution, followed by gentle pipetting and incubation at 80℃ for 5 minutes. Following the cooling, 3 µl of 4 mg/ml RNase was added to the sample, and the contents mixed. The sample was incubated at 37°C for 15 minutes and brought to room temperature. Protein precipitation was done by adding 200 µl of protein precipitation solution (Promega, Madison, WI) and vertexing for 20 seconds. The mixture was put on ice for 5 minutes and spun at 14,000 rpm for 3 minutes. Subsequently, the supernatant was transferred into a fresh tube containing 600 µl of room-temperature isopropanol, mixed, and the DNA pelleted by centrifugation at 14,000 rpm for 2 minutes. The supernatant was removed, added 600 µl of 70% ethanol, mixed by pipetting, and centrifuged for 2 minutes at 14,000 rpm. The ethanol was

removed, and the pellet air-dried for 10 minutes. The DNA pellet was rehydrated with 100 µl of rehydration solution from Promega, Madison, WI, and incubated overnight at 4°C.

3.3 Growth Curves

The mutant and wild-type *S. maltophilia 02* cultures were grown overnight in LB broth at 30°C in a roller The following cultures were made to perform the above experiments. For the streak plate, a single colony was inoculated into 5 ml of LB broth. Then, 80 µl of kanamycin was added to the mutant culture. Afterward, the cultures were incubated at 30°C for 18 hours on a roller drum. The next day, for the *S. maltophilia 02* and the AX55 mutant, two test tubes with 9.5 ml of LB broth and 500 µl of the overnight culture were set up. In the mixture, the uniformity of the medium was ensured before it was divided into two test tubes each having a volume of 5 ml comprising a mix of 4.75 ml LB broth and 250 µl of overnight culture. The test tubes were labeled appropriately. Two test tubes for *S. maltophilia 02*—one with and one without selenite, and similarly two test tubes for AX55—one with and one without the addition of selenite, so at the end, four test tube samples were prepared for the growth curve experiment.

Cell culture readings were taken with a NanoDrop 8000, with a cuvette, using 100 µl of cells in each measurement. Zeroing was performed using the device with 100 µl of LB broth. The culture tubes were stored in the roller drum at 30°C to maintain a constant temperature. To ensure the accuracy of the measurements taken, only one tube could be removed from the roller drum at any time for reading to avoid cooling the cells. After an incubation of 90 minutes, sodium selenite was added to the experimental tubes to a final concentration of 10 mM, and equal volume of water was added to the positive control tubes. Measurement for all four growth curve samples was done every

30 minutes till 5 hours and 60 minutes following 5 hours, for 720 minutes. Seven growth curves were taken to maintain normalization of data.

3.4 Total RNA Preparation

RNA was extracted from 200 µl of cell culture. All these samples were collected at time variables- two samples were collected after the incubation period of 90 minutes before the addition of selenite, four samples were collected 2 hours after the addition of sodium selenite, and another four RNA samples were collected 3 hours post-addition of sodium selenite. In total, there were 10 samples for RNA purification. Different samples at the time points are mentioned in Table 1 below for reference.

Table 1-RNA samples

RNA	90 minutes	210 minutes	270 minutes
S02	S02 -no selenite	S02- water S02- selenite	S02- water S02- selenite
AX55	AX55- no selenite	AX55- water AX55- selenite	AX55- water AX55- selenite

The following day, pellets were thawed and resuspended in 110 µL of a TE buffer mixture. This was prepared by adding 10 µL of proteinase K with 100 µL of a TE buffer containing 15 mg/mL lysozyme. In each sample, the constituents of the buffer were 45 µL proteinase K, 450 µL TE buffer, and 6.75 mg lysozyme. The cells were resuspended and then incubated at room temperature

for 10 minutes, with vertexing for 10 seconds every 2 minutes. Afterward, each sample was added to 350 µL of RLT buffer with 10 µL of β-mercaptoethanol per mL of RLT buffer. The total volume equaled 1.575 mL of RLT and 1.58 µL of β-mercaptoethanol.

After incubation, the samples were centrifuged at 10,000 rpm for 2 minutes, then the supernatant was transferred to new 1.7 ml tubes with 250 µl of 100% ethanol. These mixtures were loaded onto RNA spin columns and then centrifuged for 30 seconds to bind the RNA to the columns. The flowthrough was then discarded and 700 µl of Buffer RW1 was added to each spin column.

The columns were then centrifuged at 10,000 rpm for 30 seconds and the flow-through was discarded. The columns were washed twice with 500 µl of Buffer RPE (QIAGEN, Germantown, MD), for 30 seconds and then for 2 minutes. Following each wash step, the flow-through was discarded. Finally, 1 minute of centrifugation at 10,000 rpm without buffer was performed to remove any residual wash solutions. Afterward, spin columns were transferred into new 1.5 ml collection tubes. RNA was eluted with 30 µl RNase-free water from QIAGEN, Germantown, MD. Elution was repeated with each column spun through at a speed of 1,000 rpm for 90 seconds. The eluted RNA was transferred into four separate 0.65 ml microfuge tubes, after which the concentration of RNA in each was measured using a NanoDrop 8000.

3.5 cDNA Synthesis

The RNA was reverse transcribed into cDNA according to the procedure. First, 100 ng of RNA was adjusted for each sample and then nuclease-free water was added to each in a final volume of 6 µl. Afterward, 2 µl of Random Primer Mix from New England BioLabs, Ipswich, MA, was added to each sample and brought up to a volume of 8 µl. Also, the setting up of a negative control tube for each RNA sample was performed. Denaturation of the RNA and primer mixtures was

performed in a thermocycler at 65°C for 5 minutes. Afterward, the tubes were placed on ice before the addition of 10 µl of ProtoScript II Reaction Mix (New England BioLabs). The control tubes contained 2 µl of nuclease-free water, while the experiment tubes contained 2 µl of ProtoScript II Enzyme Mix. Following this, cDNA synthesis was carried out by thermocycler as follows:

25°C for 5 minutes, 42°C for 60 minutes, and 80°C for 5 minutes, followed by holding at 4°C.

Each PCR reaction contained 1 µl of the cDNA.

3.6 Primers

Custom DNA oligonucleotides were designed using Benchling software and ordered from IDT DNA Technologies in Coralville, Iowa for synthesis.

Table 2- Primers

Primers	Sequence	
MetK2F	AAGGTCATCACGGACATCGG	DNA
MetK2R	TTCTTCGGGCTTCTTGCGAT	DNA
S02_GAPDH_F	AAACCGCGCAGAAGCACATCGA	
S02_GAPDH_R	GCCGGCGTAGGTCTTGTCGTTC	

3.7 PCR Amplification

Primers targeting the sequences of interest were primarily designed using Benchling, targeting the selenite-resistant bacteria outer membrane proteins. Briefly, the pellets of the primers were centrifuged for 10 seconds and resuspended to a final concentration of 100 µM in TE buffer. The solution was prepared in the TE buffer containing 10 mM Tris-HCl, pH 8.0, and 1 mM EDTA, both obtained from Amresco, Solon, OH. Thereafter, a 10 µM working stock was prepared by mixing 10 µl of the dissolved primer with 90 µl of nuclease-free. A list of primers is mentioned above in Table 2 for reference.

GoTaq Green polymerase was used to carry out different PCR reactions that were obtained from Promega located in Madison, WI. Stock primers of 100 µM were diluted to a final concentration of 4 µM. This was done by mixing 4 µl of the primer with 96 µl of nuclease-free water.

Afterward, the reaction mix was prepared that involved 10 µl of 2x GoTaq Green polymerase, 2.5 µl of forward primer, 2.5 µl of reverse primer, 4 µl of nuclease-free water, and 1 µl of the template. The PCR reaction was done. The PCR program is as follows: -

1. Run 1 cycle for 2 minutes at 95℃.
2. Run 30 cycles for 1 minute at 95 ℃.
3. Run 30 cycles for 1 minute at 60 ℃.
4. Run 30 cycles 30 sec at 72 ℃
5. Run 1 cycle for 10 min at 72 ℃

6. 25 ℃ hold

Table 3- Templates for PCR reaction

Template	90 min	210 min	270 min
cDNA S02	cDNA S02-No Se	cDNA S02-No Se cDNA S02-Se	cDNA S02-No Se cDNA S02-Se
cDNA AX55	cDNA AX55-No Se	cDNA AX55-No Se cDNA AX55-Se	cDNA AX55-No Se cDNA AX55-Se
Genomic S02	Genomic S02	Genomic S02	Genomic S02
Genomic AX55	Genomic AX55	Genomic AX55	Genomic AX55

3.8 Agarose Gel Electrophoresis

To make 1% agarose gel, 1.3 grams of BioExcell Agarose LE from WorldWide Medical Products was combined with 130 ml of 1x TBE buffer from Amresco, which contained 0.089 M Tris Base, 0.089 M Borate, and 0.002 M EDTA. Mix well and heat in the microwave until the agarose is fully dissolved. Then add 13 µl of Gel Green Nucleic Acid Stain , using Embi Tec's product, diluted 1:10,000 from its stock solution. Stir the solution with a stir bar on a stir plate. Pour into a gel tray

and let it harden for about 30 minutes with the combs inserted to form wells. Once hardened, remove the combs. The gels were then prepared in a RunOne Electrophoresis System from Embi Tec, San Diego, CA, and overlayed with 1x TBE buffer. The PCR product was added with 6X loading dye. DNA separation was performed at 100V subsequently. The process was stopped when the bromophenol blue dye had reached the bottom of the gel. The visualizations were performed in a PrepOne Sapphire illuminator with an Embi Tec camera.

CHAPTER IV: RESULTS

4.1 Growth Curves

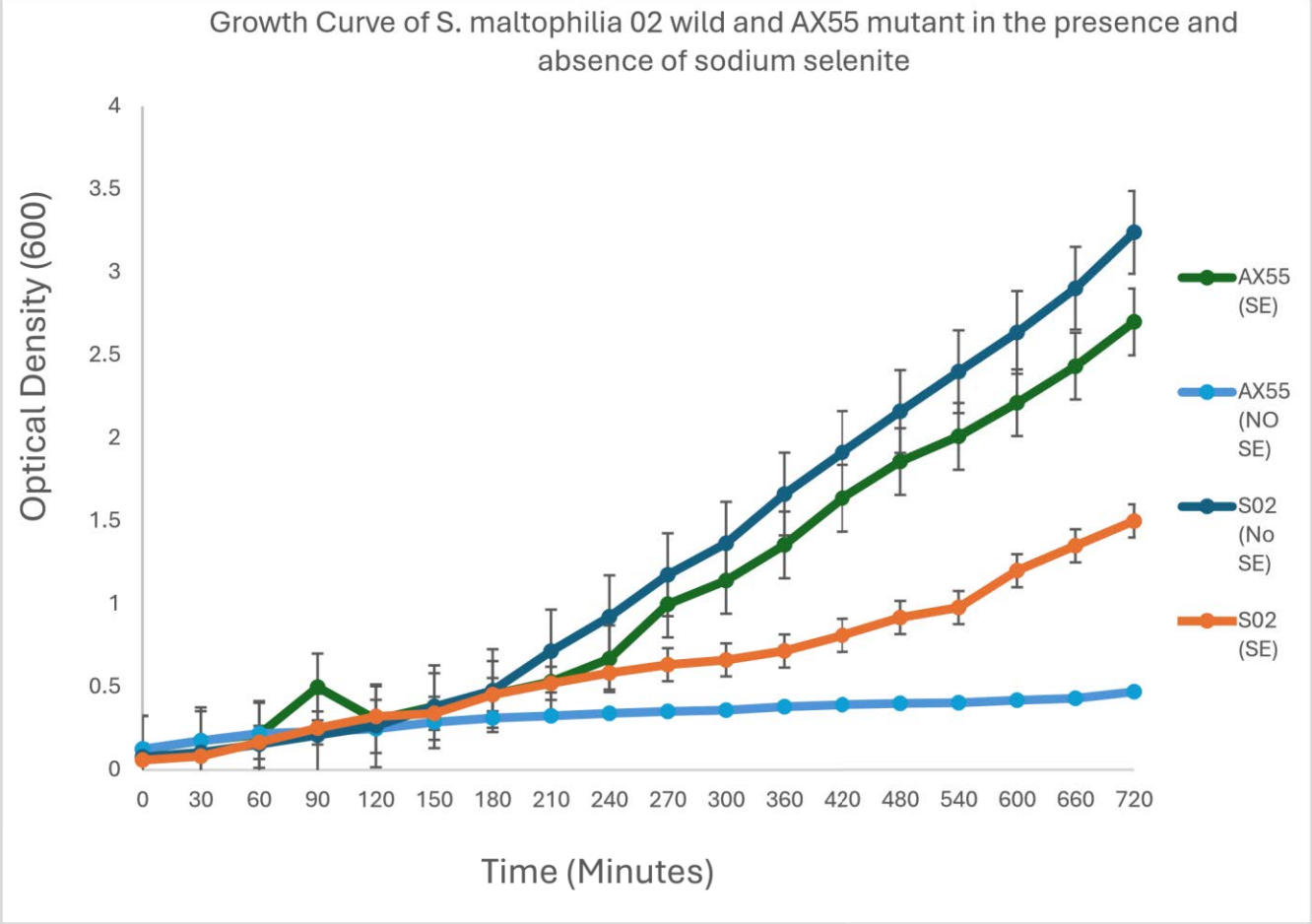

Figure 1- Growth Curve of *S. maltophilia 02* and mutant AX55

The growth of Stenotrophomonas *maltophilia* 02 (wild type) and AX55 (mutant) in rich LB broth were monitored over twelve hours, under aerobic conditions at 37°C. Cell density was measured using optical density at 600 nm. Four growth curves were studied for two different strains in the presence and absence of sodium selenite.

1. Growth Curve of S. *maltophilia 02* without Sodium Selenite

The lag phase lasted for about 120 minutes, in which there was no increase in OD600, thus it was an adjustment period for the bacteria. The exponential, or log, phase started at about the 120minute mark and lasted for 720 minutes in which OD600 increased significantly, thus showing that the cells were undergoing active cell division. The maximum OD600 of 3.24 was at 12 hours.

2. Growth Curve of *S. maltophilia 02* with Sodium Selenite

The lag phase of the *S. maltophilia 02* population in the presence of sodium selenite was 90 minutes, followed by an exponential phase that lasted 720 minutes. The maximum OD600 reached was 1.5 at 720 minutes, where the growth was significantly inhibited compared to having no sodium selenite.

3. Growth Curve of AX55 without Sodium Selenite

The lag phase for AX55 without sodium selenite, lasted 180 minutes. The exponential phase lasted for 720 minutes, with a maximum OD600 realized at 12 hours with a value of 2.54.

4. Growth Curve of AX55 With Sodium Selenite

For AX55 with added sodium selenite, the lag phase lasted 120 minutes before the growth remained flat up to 720 minutes at an OD600 of 0.41.

There was more growth of the wild-type *S. maltophilia 02* compared with the AX55 mutant both in the absence and presence of sodium selenite. A depression in OD600 was observed for both strains on the addition of sodium selenite; more reduction was noted for AX55. AX55 growth in the exponential phase was stagnant. The growth curves indicate that for *S. maltophilia 02* without selenite, AX55 without selenite, and *S. maltophilia 02* with selenite the growth phase may last for more than 18 hours before entering the decline phase. In sharp contrast, the log phase for mutant

AX55 in the presence of sodium selenite extended beyond 18 hours. The error bar for the graph signifies deviation in seven data that was collected after normalization of data.

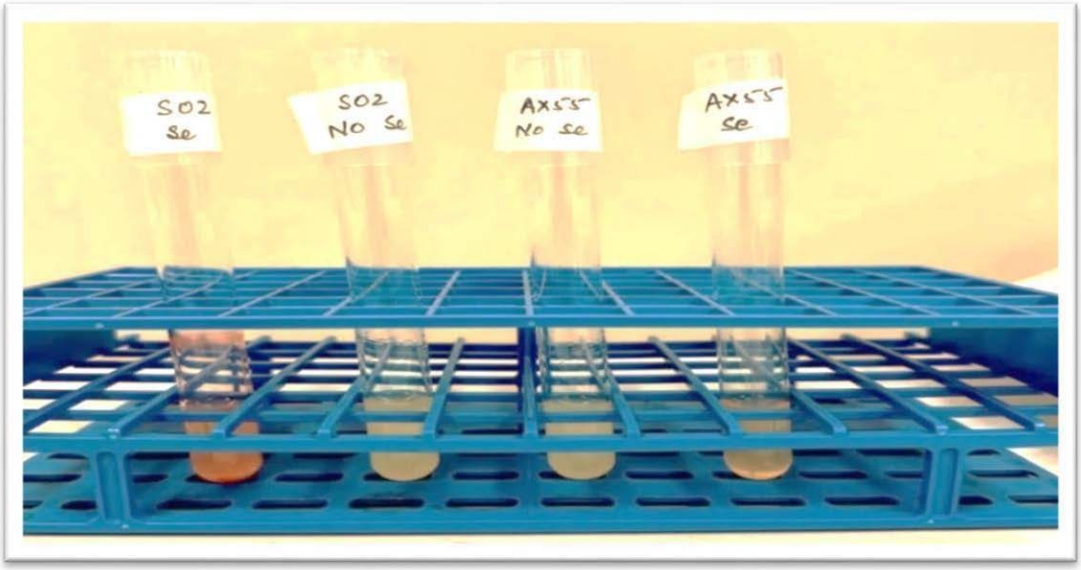

Figure 2- Sodium Selenite supplementation to LB cell cultures

In the setup of this experiment, the reduction of selenite to elemental selenium is indicated by the formation of a red precipitate. This red coloration would correspond to the existence of elemental selenium. Using the wild-type *S. maltophilia 02*, there would form a certain observable amount of red precipitate, thus indicative of a decent reduction. On the other hand, the mutant AX55 had very weak red coloration, so in this case, the reduction of selenite to elemental selenium will be significantly lower.

4.2 Agarose Gel Electrophoresis

Primers	90	DNA	C
GAPDH		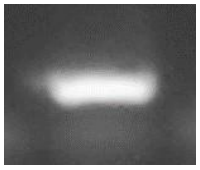	
metK	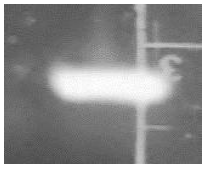	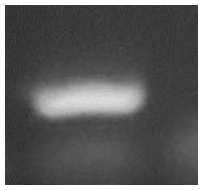	

Figure 3: Expression levels of GAPDH and metK genes *in S. maltophilia 02* at 90 minutes before sodium selenite addition. Agarose Gel, 1% electrophoresis of the RT-PCR products amplified using primers MetK2F/MetK2R and S02_GAPDH_F/S02_GAPDH_R that are specific to the GAPDH and metK genes respectively.

As shown in Fig 3. In the cDNA separation of *S. maltophilia* 02 using GAPDH and *metK* primer, DNA refers to Genomic DNA as positive control and C as negative control with nuclease water. For transcriptional differences in *S. maltophilia* 02, PCR was performed. Here, genomic DNA served as the reference or positive control, while nuclease-free water was a negative control. In the 1% agarose gel electrophoresis, resolved at 100V for 45 minutes, there were distinct bands for both GAPDH and *metK* primers. No difference in the transcriptional level could be observed between

the GAPDH and *metK* primer on the gel images hence, these genes are supposedly equally transcriptionally active under such conditions. Control reactions further confirmed the specificity and reliability of the PCR process, showing that, before treatment with selenite, transcriptional levels of GAPDH and *metK* in *S. maltophilia 02* are equivalent

Primers	120	180	DNA	C
GAPDH-No selenite	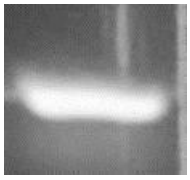			
GAPDH-Selenite			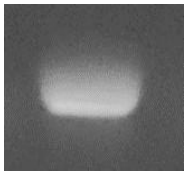	
metK-No selenite		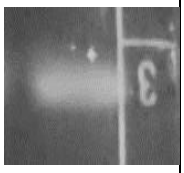	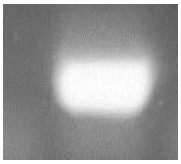	

Figure 4: Expression levels of GAPDH and *metK* genes in *S. maltophilia* 02 at 120 minutes and 180 minutes following sodium selenite addition. Agarose Gel, 1% electrophoresis of the RT-PCR

products amplified using primers MetK2F/MetK2R and S02_GAPDH_F/S02_GAPDH_R that are specific to the GAPDH and metK genes respectively.

The results of the gel electrophoresis in Fig. 4 indicated the separation of *S. maltophilia* 02 cDNA with GAPDH and *metK* primers at 120- and 180 minutes post sodium selenite addition. Genomic DNA was used as the positive control; on the other hand, nuclease-free water acted as the negative control. As evident in this analysis, no notable differences in transcription between the GAPDH and *metK* primers were found, thereby signifying the expression of these genes. However, bands at 120 minutes are more intensified compared with those at the 180-minute time point, thus representing a clearer transcriptional response or number of copies.

Primers	90	DNA	C
GAPDH	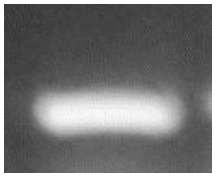	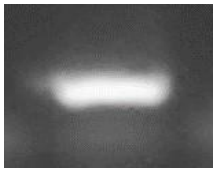	
metK	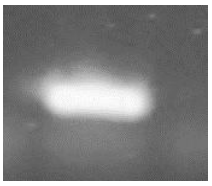		

Figure 5: Expression of the GAPDH and *metK* gene in mutant AX55 at 90 minutes before adding sodium selenite. Agarose gel (1%) electrophoresis of the RT-PCR products obtained using primers MetK2F, MetK2R, S02_GAPDH_F and S02_GAPDH_R specific for GAPDH and *metK* gene

Fig 5. depicts the separation of cDNA from *S. maltophilia*. 02 mutant AX55 with GAPDH and *metK* primers. Genomic DNA was used as the positive control while nuclease-free water served as the negative control. Gel electrophoresis revealed distinct bands for the two primers, GAPDH and *metK*. There was no significant difference in transcriptional levels with the GAPDH and *metK* primers, indicating that these genes are expressed similarly under such conditions. Control reactions confirmed the specificity and accuracy of the PCR, showing that transcriptional levels of GAPDH and *metK* in AX55 were equal before the addition of selenite.

Primers	120	180	DNA	C
GAPDH-No selenite	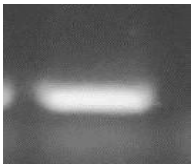	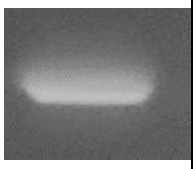		
GAPDH-Selenite	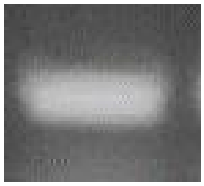			

metK-No selenite	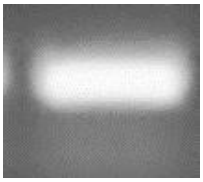	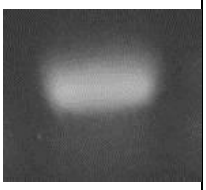		
metK-Selenite				

Figure 6: Expression levels of GAPDH and *metK* genes in AX55 at 120 minutes and 180 minutes following sodium selenite addition. Agarose Gel, 1% electrophoresis of the RT-PCR products amplified using primers MetK2F/MetK2R and S02_GAPDH_F/S02_GAPDH_R that are specific for GAPDH and *metk*

The result shows genomic DNA was used as a positive control whereas nuclease-free water was used as a negative control. There was no differentiation in the transcriptional levels of AX55 between the GAPDH and *metK* primers, so their gene expression is considered the same. However, the bands at 120 minutes were more in without selenite than with selenite. All band's 180 minutes showed the same intensity both with and without selenite.

The overall analysis of RT-PCR showed that there are no significant differences in *metK* gene expression with mutant or wild-type strains, so some other factor could be interfering with the role of the transposon in selenite resistance or methylation; however, promoter prediction is inconclusive. GAPDH was used as a control for checking the reliability of transcriptional

measurements and proved to be constantly expressed in all samples, hence proving the reliability of the transcriptional data obtained in the study.

1.3 Multiple sequence alignment

Multiple sequence alignment of S-adenosylmethionine synthetase from AX55 and 20 homologs retrieved for comparison was performed. For this, the MUSCLE function in the UGENE tool was used. (102).

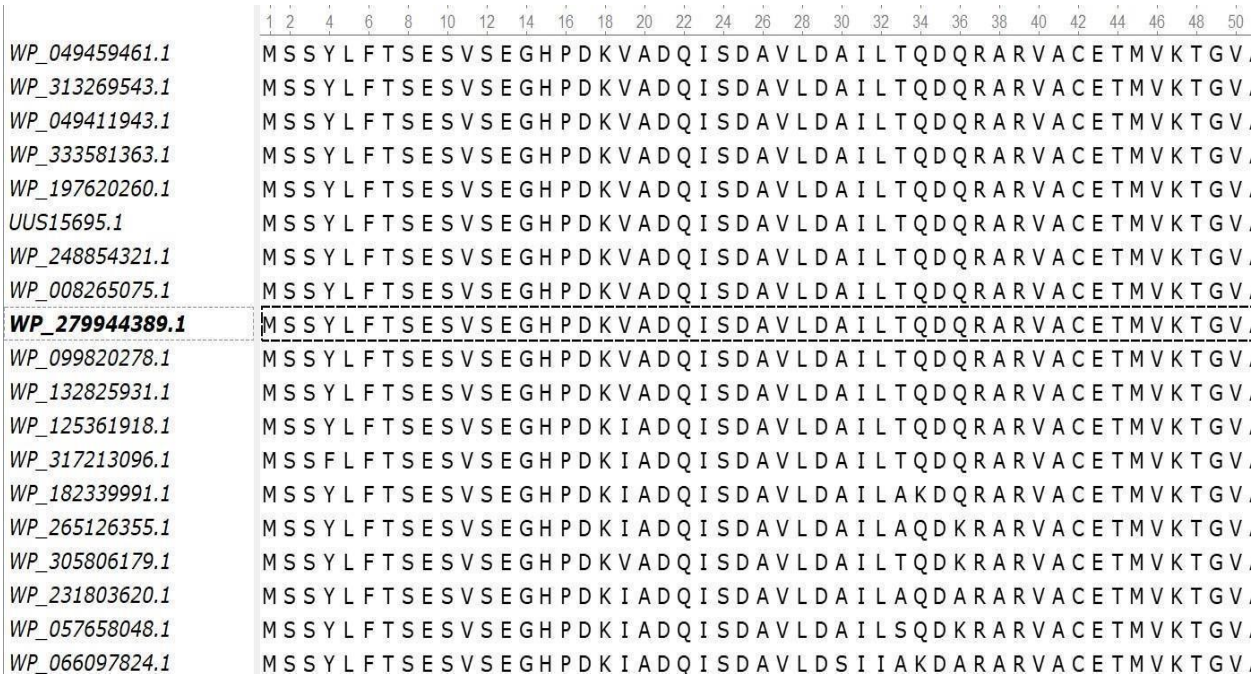
1 2 4 6 8 10 12 14 16 18 20 22 24 26 28 30 32 34 36 38 40 42 44 46 48 50
WP_049459461.1 MSSYLFTSESVSEGHPDKVADQISDAVLDAILTQDQRARVACETMVKTGV
WP_313269543.1 MSSYLFTSESVSEGHPDKVADQISDAVLDAILTQDQRARVACETMVKTGV
WP_049411943.1 MSSYLFTSESVSEGHPDKVADQISDAVLDAILTQDQRARVACETMVKTGV
WP_333581363.1 MSSYLFTSESVSEGHPDKVADQISDAVLDAILTQDQRARVACETMVKTGV
WP_197620260.1 MSSYLFTSESVSEGHPDKVADQISDAVLDAILTQDQRARVACETMVKTGV
UUS15695.1 MSSYLFTSESVSEGHPDKVADQISDAVLDAILTQDQRARVACETMVKTGV
WP_248854321.1 MSSYLFTSESVSEGHPDKVADQISDAVLDAILTQDQRARVACETMVKTGV
WP_008265075.1 MSSYLFTSESVSEGHPDKVADQISDAVLDAILTQDQRARVACETMVKTGV
WP_279944389.1 MSSYLFTSESVSEGHPDKVADQISDAVLDAILTQDQRARVACETMVKTGV
WP_099820278.1 MSSYLFTSESVSEGHPDKVADQISDAVLDAILTQDQRARVACETMVKTGV
WP_132825931.1 MSSYLFTSESVSEGHPDKVADQISDAVLDAILTQDQRARVACETMVKTGV
WP_125361918.1 MSSYLFTSESVSEGHPDKIADQISDAVLDAILTQDQRARVACETMVKTGV
WP_317213096.1 MSSFLFTSESVSEGHPDKIADQISDAVLDAILTQDQRARVACETMVKTGV
WP_182339991.1 MSSYLFTSESVSEGHPDKIADQISDAVLDAILAKDQRARVACETMVKTGV
WP_265126355.1 MSSYLFTSESVSEGHPDKIADQISDAVLDAILAQDKRARVACETMVKTGV
WP_305806179.1 MSSYLFTSESVSEGHPDKVADQISDAVLDAILTQDKRARVACETMVKTGV
WP_231803620.1 MSSYLFTSESVSEGHPDKIADQISDAVLDAILAQDARARVACETMVKTGV
WP_057658048.1 MSSYLFTSESVSEGHPDKIADQISDAVLDAILSQDKRARVACETMVKTGV
WP_066097824.1 MSSYLFTSESVSEGHPDKIADQISDAVLDSIIAKDARARVACETMVKTGV


52 54 56 58 60 62 64 66 68 70 72 74 76 78 80 82 84 86 88 90 92 94 96 98 100
WP_049459461.1 IVAGEITTSAWIDLEALTRKVITDIGYDSSDVGFDGATCGVLNLIGKQS
WP_313269543.1 IVAGEITTSAWIDLEALTRKVITDIGYDSSDVGFDGATCGVLNLIGKQS
WP_049411943.1 IVAGEITTSAWIDLEALTRKVITDIGYDSSDVGFDGATCGVLNLIGKQS
WP_333581363.1 IVAGEITTSAWIDLEALTRKVITDIGYDSSEVGFDGATCGVLNLIGKQS
WP_197620260.1 IVAGEITTSAWIDLEALTRKVITDIGYDSSDVGFDGATCGVLNLIGKQS
UUS15695.1 IVAGEITTSAWIDLEALTRKVITDIGYDSSDVGFDGATCGVLNLIGKQS
WP_248854321.1 IVAGEITTSAWIDLEALTRKVITDIGYDSSDVGFDGATCGVLNLIGKQS
WP_008265075.1 IVAGEITTSAWIDLEALTRKVITDIGYDSSEVGFDGATCGVLNLIGKQS
WP_279944389.1 IVAGEITTSAWIDLEALTRKVITDIGYDSSEVGFDGATCGVLNLIGKQS
WP_099820278.1 IVAGEITTSAWIDLEALTRKVIVDIGYDSSDVGFDGATCGVLNLIGKQS
WP_132825931.1 IVAGEITTSAWIDLEALTRKVIVDIGYDSSDVGFDGATCGVLNLIGKQS
WP_125361918.1 IVAGEITTSAWIDLEALTRKVILDIGYNSSDVGFDGATCGVLNLIGKQS
WP_317213096.1 IVAGEITTSAWIDLEALTRKVILDIGYDSSDVGFDGATCGVLNLIGKQS
WP_182339991.1 IVAGEITTSAWIDLEALTRQVILDIGYNSSDVGFDGATCGVLNLIGKQS
WP_265126355.1 IVAGEITTSAWIDLEALTRKVILDIGYDSSDVGFDGATCGVLNLIGKQS
WP_305806179.1 IVAGEITTSAWIDLEALTRKVIVDIGYDSSEVGFDGATCGVLNLIGKQS
WP_231803620.1 IVAGEITTSAWIDLEALTRKVILDIGYNSSDVGFDGATCGVLNLIGKQS
WP_057658048.1 IVAGEITTSAWIDLEALTRKVILDIGYNSSDVGFDGATCGVLNLIGKQS
WP_066097824.1 IVAGEITTSAWVDLEALTRKVILDIGYDSSDVGFDGATCGVLNLIGKQS

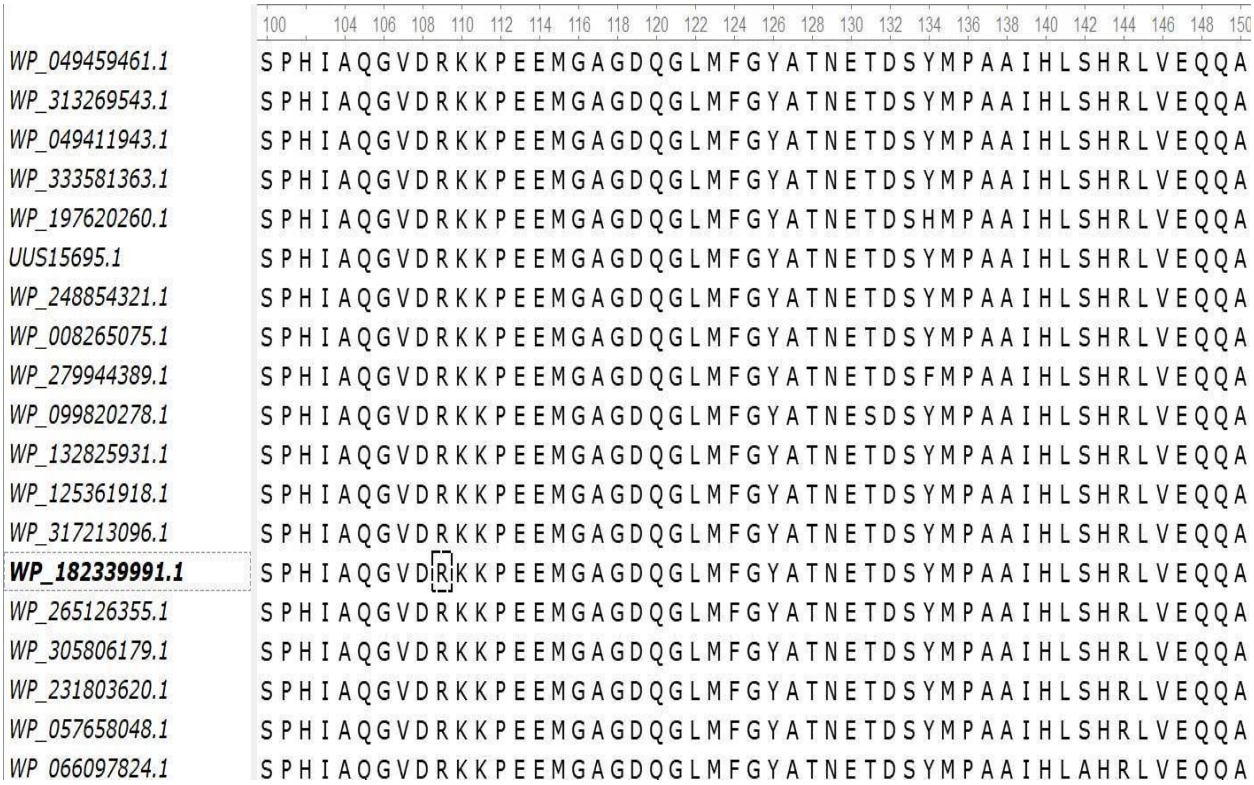
100 104 106 108 110 112 114 116 118 120 122 124 126 128 130 132 134 136 138 140 142 144 146 148 150
WP_049459461.1 SPHIAQGVDRKKPEEMGAGDQGLMFGYATNETDSYMPAAIHLSHRLVEQQA
WP_313269543.1 SPHIAQGVDRKKPEEMGAGDQGLMFGYATNETDSYMPAAIHLSHRLVEQQA
WP_049411943.1 SPHIAQGVDRKKPEEMGAGDQGLMFGYATNETDSYMPAAIHLSHRLVEQQA
WP_333581363.1 SPHIAQGVDRKKPEEMGAGDQGLMFGYATNETDSYMPAAIHLSHRLVEQQA
WP_197620260.1 SPHIAQGVDRKKPEEMGAGDQGLMFGYATNETDSHMPAAIHLSHRLVEQQA
UUS15695.1 SPHIAQGVDRKKPEEMGAGDQGLMFGYATNETDSYMPAAIHLSHRLVEQQA
WP_248854321.1 SPHIAQGVDRKKPEEMGAGDQGLMFGYATNETDSYMPAAIHLSHRLVEQQA
WP_008265075.1 SPHIAQGVDRKKPEEMGAGDQGLMFGYATNETDSYMPAAIHLSHRLVEQQA
WP_279944389.1 SPHIAQGVDRKKPEEMGAGDQGLMFGYATNETDSFMPAAIHLSHRLVEQQA
WP_099820278.1 SPHIAQGVDRKKPEEMGAGDQGLMFGYATNESDSYMPAAIHLSHRLVEQQA
WP_132825931.1 SPHIAQGVDRKKPEEMGAGDQGLMFGYATNETDSYMPAAIHLSHRLVEQQA
WP_125361918.1 SPHIAQGVDRKKPEEMGAGDQGLMFGYATNETDSYMPAAIHLSHRLVEQQA
WP_317213096.1 SPHIAQGVDRKKPEEMGAGDQGLMFGYATNETDSYMPAAIHLSHRLVEQQA
WP_182339991.1 SPHIAQGVDRKKPEEMGAGDQGLMFGYATNETDSYMPAAIHLSHRLVEQQA
WP_265126355.1 SPHIAQGVDRKKPEEMGAGDQGLMFGYATNETDSYMPAAIHLSHRLVEQQA
WP_305806179.1 SPHIAQGVDRKKPEEMGAGDQGLMFGYATNETDSYMPAAIHLSHRLVEQQA
WP_231803620.1 SPHIAQGVDRKKPEEMGAGDQGLMFGYATNETDSYMPAAIHLSHRLVEQQA
WP_057658048.1 SPHIAQGVDRKKPEEMGAGDQGLMFGYATNETDSYMPAAIHLSHRLVEQQA
WP_066097824.1 SPHIAQGVDRKKPEEMGAGDQGLMFGYATNETDSYMPAAIHLAHRLVEQQA

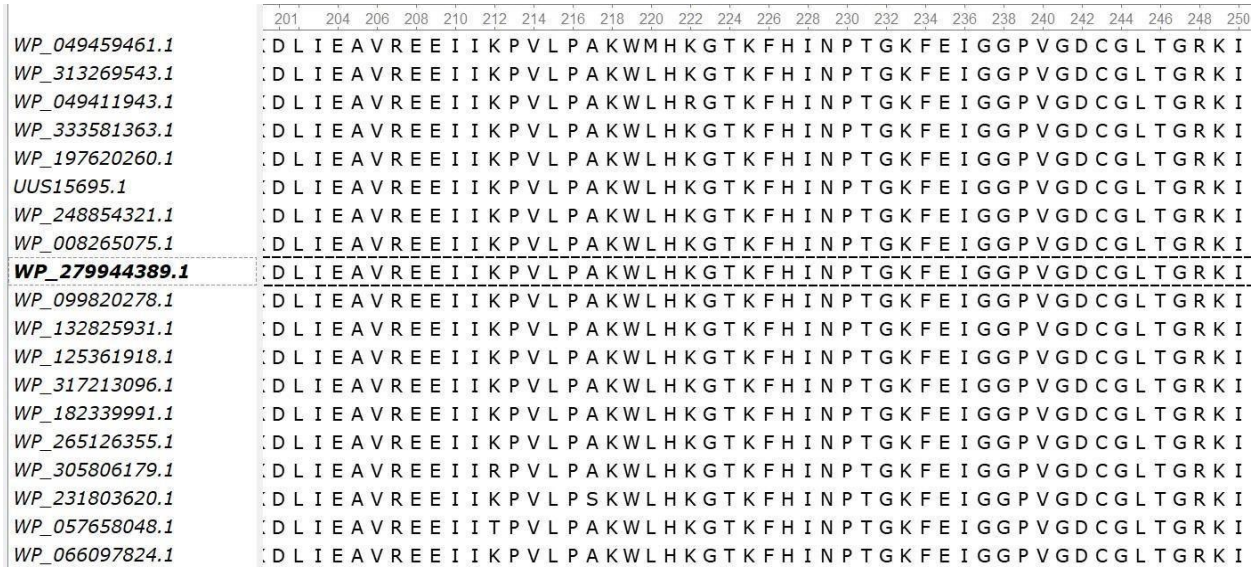
201 204 206 208 210 212 214 216 218 220 222 224 226 228 230 232 234 236 238 240 242 244 246 248 250
WP_049459461.1 DLIEAVREEIIKPVLPAKWMHKGTKFHINPTGKFEIGGPVGDCGLTGRKI
WP_313269543.1 DLIEAVREEIIKPVLPAKWLHKGTKFHINPTGKFEIGGPVGDCGLTGRKI
WP_049411943.1 DLIEAVREEIIKPVLPAKWLHRGTKFHINPTGKFEIGGPVGDCGLTGRKI
WP_333581363.1 DLIEAVREEIIKPVLPAKWLHKGTKFHINPTGKFEIGGPVGDCGLTGRKI
WP_197620260.1 DLIEAVREEIIKPVLPAKWLHKGTKFHINPTGKFEIGGPVGDCGLTGRKI
UUS15695.1 DLIEAVREEIIKPVLPAKWLHKGTKFHINPTGKFEIGGPVGDCGLTGRKI
WP_248854321.1 DLIEAVREEIIKPVLPAKWLHKGTKFHINPTGKFEIGGPVGDCGLTGRKI
WP_008265075.1 DLIEAVREEIIKPVLPAKWLHKGTKFHINPTGKFEIGGPVGDCGLTGRKI
WP_279944389.1 DLIEAVREEIIKPVLPAKWLHKGTKFHINPTGKFEIGGPVGDCGLTGRKI
WP_099820278.1 DLIEAVREEIIKPVLPAKWLHKGTKFHINPTGKFEIGGPVGDCGLTGRKI
WP_132825931.1 DLIEAVREEIIKPVLPAKWLHKGTKFHINPTGKFEIGGPVGDCGLTGRKI
WP_125361918.1 DLIEAVREEIIKPVLPAKWLHKGTKFHINPTGKFEIGGPVGDCGLTGRKI
WP_317213096.1 DLIEAVREEIIKPVLPAKWLHKGTKFHINPTGKFEIGGPVGDCGLTGRKI
WP_182339991.1 DLIEAVREEIIKPVLPAKWLHKGTKFHINPTGKFEIGGPVGDCGLTGRKI
WP_265126355.1 DLIEAVREEIIKPVLPAKWLHKGTKFHINPTGKFEIGGPVGDCGLTGRKI
WP_305806179.1 DLIEAVREEIIRPVLPAKWLHKGTKFHINPTGKFEIGGPVGDCGLTGRKI
WP_231803620.1 DLIEAVREEIIKPVLPSKWLHKGTKFHINPTGKFEIGGPVGDCGLTGRKI
WP_057658048.1 DLIEAVREEIITPVLPAKWLHKGTKFHINPTGKFEIGGPVGDCGLTGRKI
WP_066097824.1 DLIEAVREEIIKPVLPAKWLHKGTKFHINPTGKFEIGGPVGDCGLTGRKI

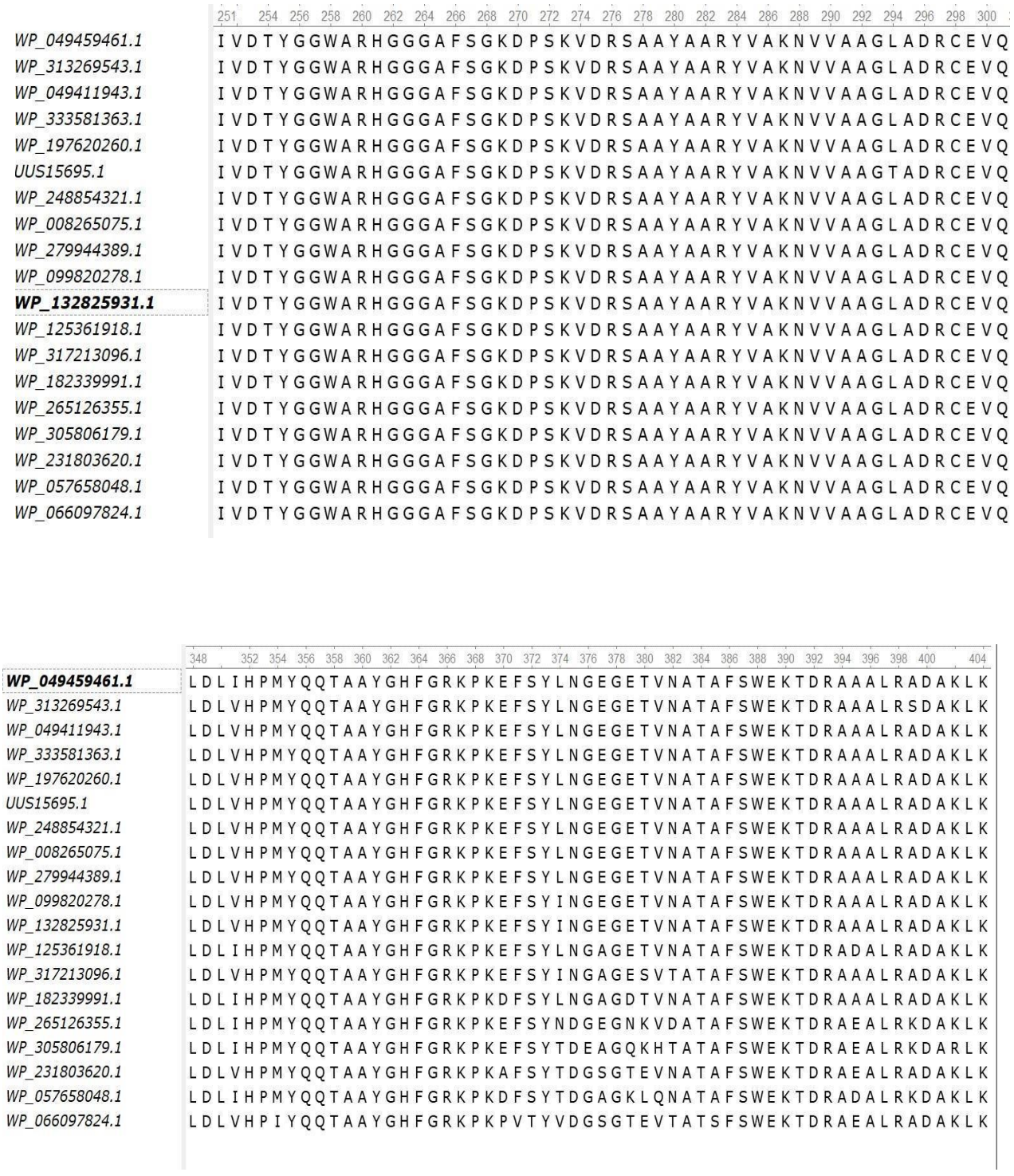

Figure 7: Multiple Sequence Alignment (102)

1.4 Phylogenetic Analysis

A phylogenetic tree was constructed to investigate the evolutionary relationship of AX55 SAM synthetase with its homologs. Sequences were imported into MEGA7 and realigned using MUSCLE for more accurate results (102-104). Maximum likelihood analysis inferred evolutionary history for each taxon and included 1000 bootstrap replicates. The percentages indicating the number of times each clade appeared in the 1000 bootstrap replicates are shown on the tree. The tree clearly shows the closeness in the evolutionary relationship between the *S. maltophilia 02* mutant and the other species of *S. maltophilia.*

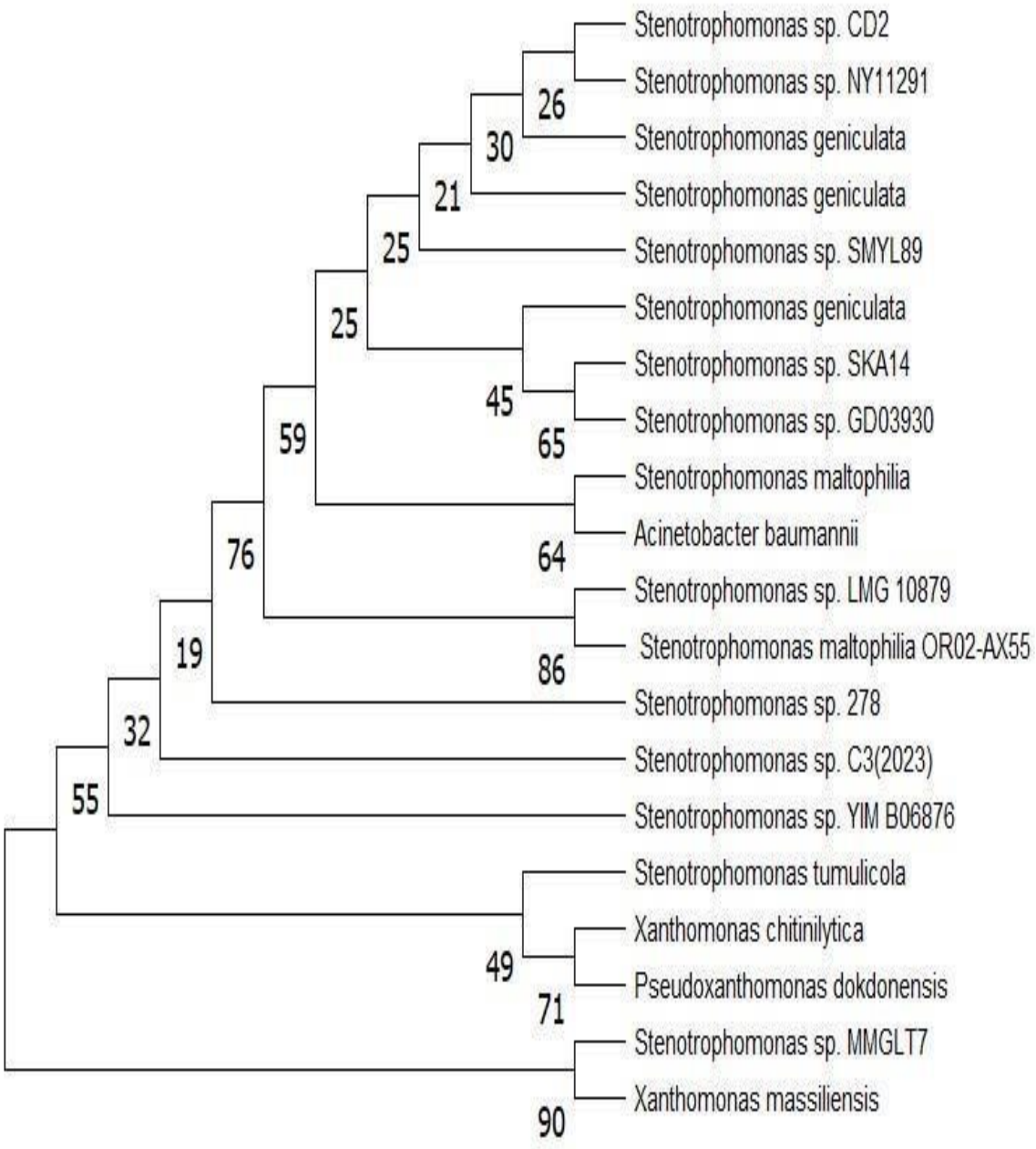

Figure 8: The phylogenetic tree describes the evolutionary relationships of AX55 S-adenosyl methionine synthetase with its closely related homologs. Branch lengths are measured in the number of amino acid substitutions per site. Bootstrap values are shown in percentage

Chapter V: Discussion

The growth patterns of wild-type *S. maltophilia 02* and mutant AX55 took a very different route. In comparison, while the mutant showed very slow growth during the exponential phase, it finally reached a plateau in growth rate. For the wild type, there was no such phenomenon in the presence of sodium selenite - it just continued to grow gradually. This is accompanied by a red precipitate of elemental selenium and a smell of garlic., which was more evident in the wild *S. maltophilia 02 compared with mutant AX55* in addition to sodium selenite.

The presence of transposon insertion at the *metK* region does cast doubts on the sensitivity of the mutant to selenite. Although the transposon is inserted into the 5' UTR rather than a coding region— which Sapphire predicts should not disrupt *metK* expression—it had been presumed that *metK* transcriptional levels in mutant AX55 would be absent than in wild *S. maltophilia 02*. In contrast to expectations, *metK* transcript levels were virtually identical in both mutant and wild types. The observation suggests that, even in the presence of sodium selenite, the expression of *metK* remains unaffected by the insertion of the transposon.

Since this is just a single experiment, it needs to be repeated to verify the results obtained. In addition, to further confirm the results obtained, a set of follow-up experiments needs to be planned and executed. For example, Western blotting techniques could be carried out for the expression of proteins. This would be realized by purifying the *metK* protein, preparing a specific mouse antibody against it, and then using SDS-PAGE to separate the proteins from cell samples. The proteins could be transferred to a blotting membrane and probed with the antibody to detect *metK* presence and levels.

Furthermore, the knockout of the *metK* gene by homologous recombination would give a much more definitive way of proving the involvement of *metK* in the observed phenotypes. Any changes

in sensitivity to sodium selenite will be observed as a direct consequence of the loss of *metK* function. Such extra techniques at their disposal will enhance the solidity and accuracy of conclusions on the function and expression of the *metK* gene in response to sodium selenite.

Microbial activities transform the selenium species and change its physical state. The alkylation of dissolved selenate or selenite can produce volatile gases such as dimethyl selenide and dimethyl diselenide (105). However, the specific enzymes involved in microbial selenium alkylation remain largely unidentified. Despite this, studies have demonstrated the potential for microbial communities to mediate selenium alkylation and volatilization, contributing to selenium detoxification (93).

Previous studies in conjunction with current findings, provide further support for the complexity of the selenium methylation mechanism. However, the following limitations of the study may be accounted for result shall be considered. First, the accuracy of RT-PCR reactions may repeat several times. Second, there could be DNA contamination in the reaction mixture that may affect the results. Third, reducing the number of PCR cycles to less than thirty cycles might show *metK* expression differences between mutant and wild-type strains that were not detected in the present study.

Chapter VI: Conclusion

In conclusion, S-adenosylmethionine is not involved in selenite resistance however other variables that regulate *metK* transcription may be involved. This work may contribute to our understanding of the intricate regulatory system of Selenite methylation.

Chapter VI: Appendices

Appendix A: Accession numbers of bacterial species used in phylogenetic analysis

Species	Accession Number
Escherichia coli K12	CQR82379.1
Stenotrophomonas maltophilia	WP_049459461.1
Stenotrophomonas geniculata	WP_313269543
Acinetobacter baumannii	SSM89913.1
Stenotrophomonas geniculata	WP_049411943.1
Stenotrophomonas geniculata	WP_333581363.1
Stenotrophomonas sp. SMYL89	WP_197620260.1
Stenotrophomonas sp. CD2	UUS15695.1
Stenotrophomonas maltophilia OR02	Not Submitted
Stenotrophomonas sp. NY11291	WP_248854321.1
Stenotrophomonas sp. GD03930	WP_279944389.1.1
Stenotrophomonas sp. LMG 10879	WP_099820278.1
Unclassified	WP_132825931.1

Stenotrophomonas sp. C3(2023)	WP_317213096.1
Stenotrophomonas tumulicola	WP_182339991.1
Xanthomonas chitinilytica	WP_265126355.1
Stenotrophomonas sp. YIM B06876	WP_305806179.1
Stenotrophomonas sp. MMGLT7	WP_231803620.1
Pseudoxanthomonas dokdonensis	WP_057658048.1
Xanthomonas massiliensis	WP_066097824.1

Appendix B: Expended Phylogenetic tree

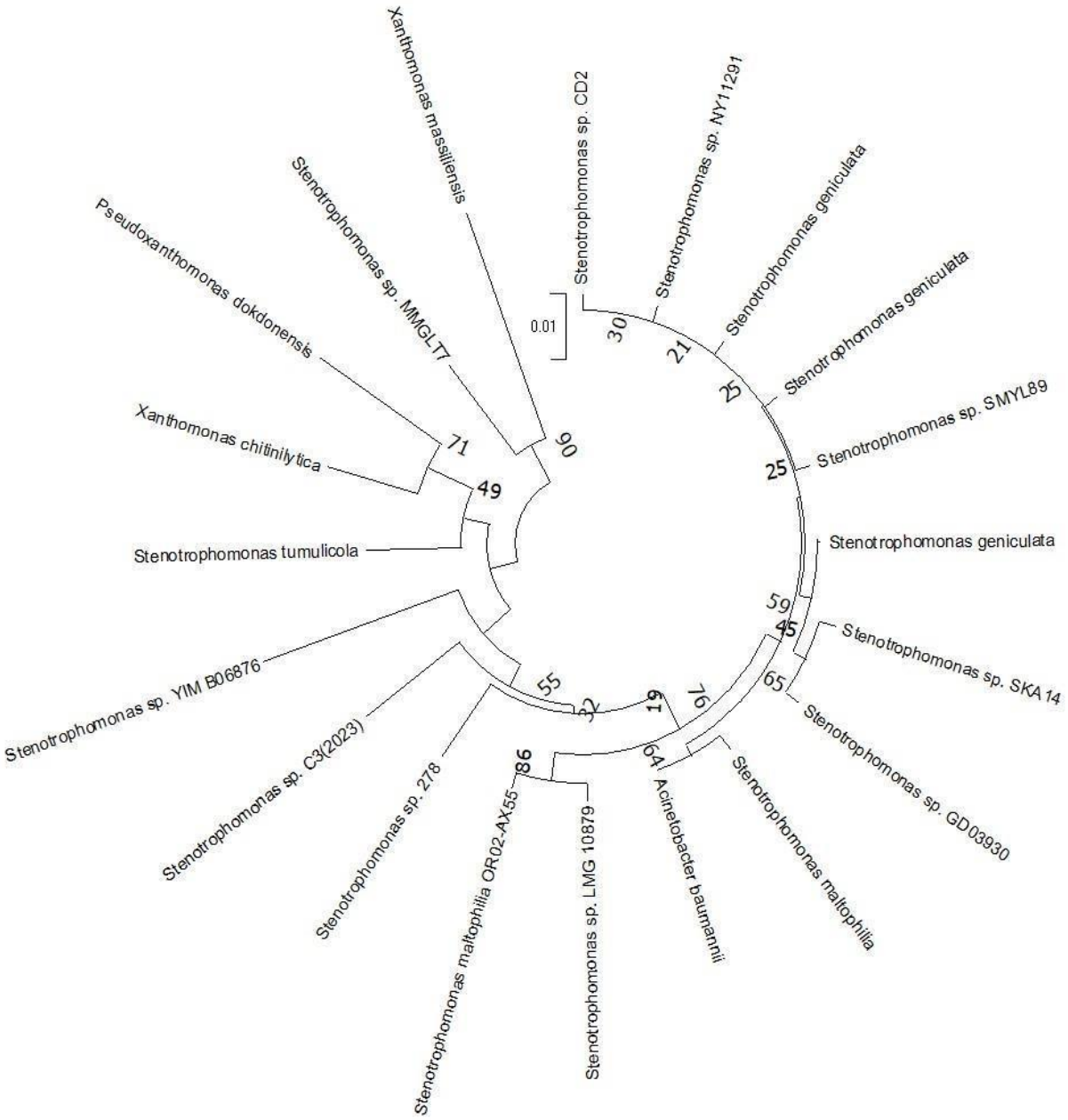
Xanthomonas massiliensis
Stenotrophomonas sp. CD2
Stenotrophomonas sp. NY11291
Stenotrophomonas geniculata
Stenotrophomonas geniculata
Stenotrophomonas sp. SMYL89
Stenotrophomonas geniculata
Stenotrophomonas sp. SKA14
Stenotrophomonas sp. GD03930
Stenotrophomonas maltophilia
Acinetobacter baumannii
Stenotrophomonas sp. LMG 10879
Stenotrophomonas maltophilia OR02-AX55
Stenotrophomonas sp. 278
Stenotrophomonas sp. C3(2023)
Stenotrophomonas sp. YIM B06876
Stenotrophomonas tumulicola
Xanthomonas chitinilytica
Pseudoxanthomonas dokdonensis
Stenotrophomonas sp. MMGLT7
0.01
30
21
25
25
59
45
65
76
64
19
86
52
55
90
49
71

Chapter VII: References

1. Rouse Campbell K, Ford CJ, and Levine DA (1998) Mercury distribution in Poplar Creek, Oak Ridge, Tennessee, USA. Environ Toxicol Chem 17:1191–1198
2. Widner, T. E., Ripple, S. R., & Buddenbaum, J. E. (1996). Identification and screening evaluation of key historical materials and emission sources at the Oak Ridge Reservation. *Health physics*, *71*(4), 457-469.
3. Brooks, S. C. (2001). Waste characteristics of the former S-3 ponds and outline of uranium chemistry relevant to NABIR Field Research Center studies. *NABIR Field Research Center, Oak Ridge, Tenn*.
4. Revis, N. W., Benson, S. B., & Osborne, T. R. (1989). *U.S. Patent No. 4,826,602*.

   Washington, DC: U.S. Patent and Trademark Office.

5. Holmes, A., Vinayak, A., Benton, C., Esbenshade, A., Heinselman, C., Frankland, D., ...

   & Caguiat, J. (2009). Comparison of two multimetal resistant bacterial strains: *Enterobacter sp. YSU* and *Stenotrophomonas maltophilia* OR02. *Current microbiology*, *59*, 526-531.
6. Adegoke, A. A., Stenström, T. A., & Okoh, A. I. (2017). *Stenotrophomonas maltophilia* as an emerging ubiquitous pathogen: looking beyond contemporary antibiotic therapy. *Frontiers in microbiology*, *8*, 2276.
7. An, S. Q., & Berg, G. (2018). *Stenotrophomonas*

maltophilia. *Trends in microbiology*, *26*(7), 637-638.

8. Geller, M., Nunes, C. P., Oliveira, L., & Nigri, R. (2018). *S. maltophilia pneumonia*: a case report. *Respiratory medicine case reports*, *24*, 44-45.
9. Rajkumari, N., Mathur, P., Gupta, A. K., Sharma, K., & Misra, M. C. (2015). Epidemiology and outcomes of *Stenotrophomonas maltophilia* and *Burkholderia cepacia* infections among trauma patients of India: a five-year experience. *Journal of Infection Prevention*, *16*(3), 103-110.
10. Gajdács, M., & Urbán, E. (2019). Prevalence and antibiotic resistance of *Stenotrophomonas maltophilia* in respiratory tract samples: a 10-year epidemiological snapshot. *Health services research and managerial epidemiology*, *6*, 2333392819870774.
11. Zhu, Y. G., Yoshinaga, M., Zhao, F. J., & Rosen, B. P. (2014). Earth abides arsenic biotransformations. *Annual Review of Earth and Planetary Sciences*, *42*(1), 443-467.
12. Nriagu, J. O. (1996). A history of global metal pollution. *Science*, *272*(5259), 223-223.
13. Chandrangsu, P., Rensing, C., & Helmann, J. D. (2017). Metal homeostasis and resistance in bacteria. *Nature Reviews Microbiology*, *15*(6), 338-350.
14. Bruins, M. R., Kapil, S., & Oehme, F. W. (2000). Microbial resistance to metals in the environment. *Ecotoxicology and environmental safety*, *45*(3), 198-207.
15. Silver, S., & Phung, L. T. (1996). Bacterial heavy metal resistance: new surprises. *Annual review of microbiology*, *50*(1996), 753-789.
16. Nies, D. H. (1999). Microbial heavy-metal resistance. *Applied microbiology and biotechnology*, *51*, 730-750.

17. Nies, D. H., & Silver, S. (1995). Ion efflux systems involved in bacterial metal resistances. *Journal of industrial microbiology*, *14*, 186-199.

18. Harrison, J. J., Ceri, H., & Turner, R. J. (2007). Multimetal resistance and tolerance in microbial biofilms. *Nature Reviews Microbiology*, *5*(12), 928-938.

19. Xu, S., Xing, Y., Liu, S., Luo, X., Chen, W., & Huang, Q. (2020). Co-effect of minerals and Cd (II) promoted the formation of bacterial biofilm and consequently enhanced the sorption of Cd (II). *Environmental Pollution*, *258*, 113774.

20. Chaturvedi, K. S., Hung, C. S., Crowley, J. R., Stapleton, A. E., & Henderson, J. P. (2012). The siderophore yersiniabactin binds copper to protect pathogens during infection. *Nature chemical biology*, *8*(8), 731-736.

21. Hao, X., Xie, P., Zhu, Y. G., Taghavi, S., Wei, G., & Rensing, C. (2015). Copper tolerance mechanisms of *Mesorhizobium amorphae* and its role in aiding phytostabilization by *Robinia pseudoacacia* in copper contaminated soil. *Environmental Science & Technology*, *49*(4), 2328-2340.

22. Das, S., Dash, H. R., & Chakraborty, J. (2016). Genetic basis and importance of metal resistant genes in bacteria for bioremediation of contaminated environments with toxic metal pollutants. *Applied microbiology and biotechnology*, *100*, 2967-2984.

23. Sher, S., & Rehman, A. (2019). Use of heavy metals resistant bacteria—a strategy for arsenic bioremediation. *Applied microbiology and biotechnology*, *103*, 6007-6021.

24. Orell, A., Navarro, C. A., Arancibia, R., Mobarec, J. C., & Jerez, C. A. (2010). Life in blue: copper resistance mechanisms of bacteria and archaea used in industrial biomining of minerals. *Biotechnology Advances*, *28*(6), 839-848.

25. Tarfeen, N., Nisa, K. U., Hamid, B., Bashir, Z., Yatoo, A. M., Dar, M. A., ... & Sayyed, R. Z. (2022). Microbial remediation: a promising tool for reclamation of contaminated sites with special emphasis on heavy metal and pesticide pollution: a review. *Processes*, *10*(7), 1358.

26. Lahiri, D., Nag, M., Dey, A., Sarkar, T., Joshi, S., Pandit, S., ... & Ray, R. R. (2022). Biofilm mediated degradation of petroleum products. *Geomicrobiology Journal*, *39*(3-5), 389-398.

27. Ianeva, O. D. (2009). Mechanisms of bacteria resistance to heavy metals. *Mikrobiolohichnyi zhurnal (Kiev, Ukraine: 1993)*, *71*(6), 54-65.

28. Megharaj, M., Venkateswarlu, K., & Naidu, R. (2014). Bioremediation.

29. Shamberger, R. (2012). *Biochemistry of selenium* (Vol. 2). Springer Science & Business Media.

30. Daniels, L. A. (1996). Selenium metabolism and bioavailability. *Biological trace element research*, *54*, 185-199.

31. Bokovay, G. (1995). Selenium and tellurium. *Can. Miner. Yearb*, *55*, 28-31.

32. Barceloux, D. G., & Vanadium, J. (1999). Toxicol. *Clin. Toxicol*, *37*(2), 239-258.

33. Dungan, R. S., & Frankenberger, W. T. (1999). Microbial transformations of selenium and the bioremediation of seleniferous environments. *Bioremediation Journal*, *3*(3), 171188.

34. Winkel, L. H., Johnson, C. A., Lenz, M., Grundl, T., Leupin, O. X., Amini, M., & Charlet, L. (2012). Environmental selenium research: from microscopic processes to global understanding.

35. Nancharaiah, Y. V., & Lens, P. N. L. (2015). Ecology and biotechnology of seleniumrespiring bacteria. *Microbiology and Molecular Biology Reviews*, *79*(1), 61-80.

36. Wells, M., & Stolz, J. F. (2020). Microbial selenium metabolism: a brief history, biogeochemistry and ecophysiology. *FEMS Microbiology Ecology*, *96*(12), fiaa209.

37. Davy, T., & Castellano, S. (2018). The genomics of selenium: Its past, present and future. *Biochimica et Biophysica Acta (BBA)-General Subjects*, *1862*(11), 2427-2432.

38. Wadhwani, S. A., Shedbalkar, U. U., Singh, R., & Chopade, B. A. (2016). Biogenic selenium nanoparticles: current status and future prospects. *Applied microbiology and biotechnology*, *100*, 2555-2566.

39. Shoeibi, S., Mozdziak, P., & Golkar-Narenji, A. (2017). Biogenesis of selenium nanoparticles using green chemistry. *Topics in Current Chemistry*, *375*, 1-21.

40. Tugarova, A. V., & Kamnev, A. A. (2017). Proteins in microbial synthesis of selenium nanoparticles. *Talanta*, *174*, 539-547.

41. Eswayah, A. S., Smith, T. J., & Gardiner, P. H. (2016). Microbial transformations of selenium species of relevance to bioremediation. *Applied and environmental microbiology*, *82*(16), 4848-4859.

42. Ojeda, J. J., Merroun, M. L., Tugarova, A. V., Lampis, S., Kamnev, A. A., & Gardiner, P. H. (2020). Developments in the study and applications of bacterial transformations of selenium species. *Critical reviews in biotechnology*, *40*(8), 1250-1264.

43. Wang, D., Rensing, C., & Zheng, S. (2022). Microbial reduction and resistance to selenium: mechanisms, applications and prospects. *Journal of hazardous materials*, *421*, 126684.

44. Stolz, J., Basu, P., & Oremland, R. (2002). Microbial transformation of elements: the case of arsenic and selenium. *International Microbiology*, *5*, 201-207.

45. Tejo Prakash, N., Sharma, N., Prakash, R., Raina, K. K., Fellowes, J., Pearce, C. I., ... & Pattrick, R. A. (2009). Aerobic microbial manufacture of nanoscale selenium: exploiting nature's bio-nanomineralization potential. *Biotechnology letters*, *31*, 1857-1862.

46. Kessi, J., Ramuz, M., Wehrli, E., Spycher, M., & Bachofen, R. (1999). Reduction of selenite and detoxification of elemental selenium by the phototrophic bacterium *Rhodospirillum rubrum*. *Applied and environmental microbiology*, *65*(11), 4734-4740.

47. Turner, R. J., Weiner, J. H., & Taylor, D. E. (1998). Selenium metabolism in *Escherichia coli*. *Biometals*, *11*, 223-227.

48. Tan, Y., Wang, Y., Wang, Y., Xu, D., Huang, Y., Wang, D., ... & Zheng, S. (2018). Novel mechanisms of selenate and selenite reduction in the obligate aerobic bacterium *Comamonas testosteroni* S44. *Journal of hazardous materials*, *359*, 129-138.

49. Elías, A. O., Abarca, M. J., Montes, R. A., Chasteen, T. G., Pérez-Donoso, J. M., & Vasquez, C. C. (2012). Tellurite enters *Escherichia coli* mainly through the PitA phosphate transporter. *Microbiology Open*, *1*(3), 259-267.

50. Vriens, B., Behra, R., Voegelin, A., Zupanic, A., & Winkel, L. H. (2016). Selenium uptake and methylation by the microalga *Chlamydomonas reinhardtii*. *Environmental science & technology*, *50*(2), 711-720.

51. Bebien, M., Chauvin, J. P., Adriano, J. M., Grosse, S., & Verméglio, A. (2001). Effect of selenite on growth and protein synthesis in the phototrophic bacterium *Rhodobacter sphaeroides*. *Applied and Environmental Microbiology*, *67*(10), 4440-4447.

52. Kessi, J., Turner, R. J., & Zannoni, D. (2022). Tellurite and Selenite: how can these two oxyanions be chemically different yet so similar in the way they are transformed to their metal forms by bacteria?. *Biological Research*, *55*.

53. Böck, A., Rother, M., Leibundgut, M., & Ban, N. (2006). Selenium metabolism in prokaryotes. *Selenium: Its molecular biology and role in human health*, 9-28.

54. Weekley, C. M., & Harris, H. H. (2013). Which form is that? The importance of selenium speciation and metabolism in the prevention and treatment of disease. *Chemical Society Reviews*, *42*(23), 8870-8894.

55. Nancharaiah, Y. V., & Lens, P. N. L. (2015). Ecology and biotechnology of seleniumrespiring bacteria. *Microbiology and Molecular Biology Reviews*, *79*(1), 61-80.

56. Ojeda, J. J., Merroun, M. L., Tugarova, A. V., Lampis, S., Kamnev, A. A., & Gardiner, P. H. (2020). Developments in the study and applications of bacterial transformations of selenium species. *Critical reviews in biotechnology*, *40*(8), 1250-1264.

57. Miralles-Robledillo, J. M., Torregrosa-Crespo, J., Martínez-Espinosa, R. M., & Pire, C. (2019). DMSO reductase family: phylogenetics and applications of extremophiles. *International Journal of Molecular Sciences*, *20*(13), 3349.

58. Newman, D. K., Ahmann, D., & Morel, F. M. (1998). A brief review of microbial arsenate respiration. *Geomicrobiology Journal*, *15*(4), 255-268.

59. Stolz J. F. and Oremland R. S. (1999). Bacterial respiration of arsenic and selenium, FEMS Microbiology Reviews, 23(5), 615–627

60. Debieux, C. M., Dridge, E. J., Mueller, C. M., Splatt, P., Paszkiewicz, K., Knight, I., ... & Butler, C. S. (2011). A bacterial process for selenium nanosphere assembly. *Proceedings of the National Academy of Sciences*, *108*(33), 13480-13485.

61. Butler, C. S. (2012). Metals, non-metals and minerals: The complexity of bacterial selenate respiration. *The Biochemist*, *34*(5), 23-27.

62. Wells, M., McGarry, J., Gaye, M. M., Basu, P., Oremland, R. S., & Stolz, J. F. (2019). Respiratory selenite reductase from *Bacillus selenitireducens* strain MLS10. *Journal of bacteriology*, *201*(7), 10-1128.

63. Avazeri, C., Turner, R. J., Pommier, J., Weiner, J. H., Giordano, G., & Vermeglio, A. (1997). Tellurite and selenate reductase activity of nitrate reductases from *Escherichia coli*: correlation with tellurite resistance. *Microbiology*, *143*, 1181-1189.

64. Zannoni, D., Borsetti, F., Harrison, J. J., & Turner, R. J. (2007). The bacterial response to the chalcogen metalloids Se and Te. *Advances in microbial physiology*, *53*, 1-312.

65. Lampis, S., & Vallini, G. (2021). Microbial reduction of selenium oxyanions: energyyielding and detoxification reactions. *Environmental technologies to treat selenium pollution: principles and engineering. London: IWA Publishing*, 101-143.

66. DeMoll-Decker, H., & Macy, J. M. (1993). The periplasmic nitrite reductase of *Thauera selenatis* may catalyze the reduction of selenite to elemental selenium. *Archives of microbiology*, *160*, 241-247.

67. Basaglia, M., Toffanin, A., Baldan, E., Bottegal, M., Shapleigh, J. P., & Casella, S. (2007). Selenite-reducing capacity of the copper-containing nitrite reductase of *Rhizobium sullae*. *FEMS microbiology letters*, *269*(1), 124-130.

68. Painter, E. P. (1941). The chemistry and toxicity of selenium compounds, with special reference to the selenium problem. *chemical reviews*, *28*(2), 179-213.

69. Ganther, H. E. (1971). Reduction of the selenotrisulfide derivative of glutathione to a persulfide analog by gluthathione reductase. *Biochemistry*, *10*(22), 4089-4098.

70. Pessentheiner, A. R., Pelzmann, H. J., Walenta, E., Schweiger, M., Groschner, L. N., Graier, W. F., ... & Bogner-Strauss, J. G. (2013). NAT8L (N-acetyltransferase 8-like) accelerates lipid turnover and increases energy expenditure in brown adipocytes. *Journal of Biological Chemistry*, *288*(50), 36040-36051.

71. Bébien, M., Lagniel, G., Garin, J., Touati, D., Verméglio, A., & Labarre, J. (2002). Involvement of superoxide dismutases in the response of *Escherichia coli* to selenium oxides. *Journal of bacteriology*, *184*(6), 1556-1564.

72. Björnstedt, M., Kumar, S., & Holmgren, A. (1992). Selenodiglutathione is a highly efficient oxidant of reduced thioredoxin and a substrate for mammalian thioredoxin reductase. *Journal of Biological Chemistry*, *267*(12), 8030-8034.

73. Kumar, S., Bjoernstedt, M., & Holmgren, A. (1992). Selenite is a substrate for calf thymus thioredoxin reductase and thioredoxin and elicits a large non-stoichiometric oxidation of NADPH in the presence of oxygen. *European journal of biochemistry*, *207*(2), 435-439.

74. Di Gregorio, S., Lampis, S., & Vallini, G. (2005). Selenite precipitation by a *rhizospheric* strain of *Stenotrophomonas sp*. isolated from the root system of *Astragalus bisulcatus*: a biotechnological perspective. *Environment international*, *31*(2), 233-241.

75. Piacenza, E., Presentato, A., Ambrosi, E., Speghini, A., Turner, R. J., Vallini, G., & Lampis, S. (2018). Physical–chemical properties of biogenic selenium nanostructures produced by *Stenotrophomonas maltophilia* SeITE02 and *Ochrobactrum sp*. MPV1. *Frontiers in Microbiology*, *9*, 3178.

76. Zhang, J., Taylor, E. W., Wan, X., & Peng, D. (2012). Impact of heat treatment on size, structure, and bioactivity of elemental selenium nanoparticles. *International journal of nanomedicine*, 815-825.

77. Pinel-Cabello, M., Chapon, V., Ruiz-Fresneda, M. A., Alpha-Bazin, B., Berthomieu, C., Armengaud, J., & Merroun, M. L. (2021). Delineation of cellular stages and identification of key proteins for reduction and biotransformation of Se (IV) by *Stenotrophomonas bentonitica* BII-R7. *Journal of Hazardous Materials*, *418*, 126150.

78. Ni, T. W., Staicu, L. C., Nemeth, R. S., Schwartz, C. L., Crawford, D., Seligman, J. D., ...

& Ackerson, C. J. (2015). Progress toward clonable inorganic nanoparticles. *Nanoscale*, *7*(41), 17320-17327.

79. Martínez, F. G., Moreno-Martin, G., Pescuma, M., Madrid-Albarrán, Y., & Mozzi, F. (2020). Biotransformation of selenium by lactic acid bacteria: formation of selenonanoparticles and seleno-amino acids. *Frontiers in bioengineering and biotechnology*, *8*, 506.
80. Zawadzka, A. M., Crawford, R. L., & Paszczynski, A. J. (2006). Pyridine-2, 6-bis (thiocarboxylic acid) produced by *Pseudomonas stutzeri KC* reduces and precipitates selenium and tellurium oxyanions. *Applied and Environmental Microbiology*, *72*(5), 31193129.
81. Rosenfeld, C. E., Kenyon, J. A., James, B. R., & Santelli, C. M. (2017). Selenium (IV, VI) reduction and tolerance by fungi in an oxic environment. *Geobiology*, *15*(3), 441452.
82. Eswayah, A. S., Hondow, N., Scheinost, A. C., Merroun, M., Romero-González, M., Smith, T. J., & Gardiner, P. H. (2019). Methyl selenol as a precursor in selenite reduction to Se/S species by methane-oxidizing bacteria. *Applied and environmental microbiology*, *85*(22), e01379-19.
83. Ruiz-Fresneda, M. A., Fernández-Cantos, M. V., Gómez-Bolívar, J., Eswayah, A. S., Gardiner, P. H., Pinel-Cabello, M., ... & Merroun, M. L. (2023). Combined bioreduction and volatilization of SeVI by Stenotrophomonas bentonitica: Formation of trigonal selenium nanorods and methylated species. *Science of the Total Environment*, *858*, 160030.

84. Winkel, L. H., Vriens, B., Jones, G. D., Schneider, L. S., Pilon-Smits, E., & Bañuelos, G. S. (2015). Selenium cycling across soil-plant-atmosphere interfaces: a critical review. *Nutrients*, *7*(6), 4199-4239.

85. Doran, J. W., & Alexander, M. (1977). Microbial transformations of selenium. *Applied and* Environmental *Microbiology*, *33*(1), 31-37.

86. Chasteen TG. 1993. Confusion between dimethyl selenenyl sulfide and dimethyl selenone released by bacteria. Appl Organometal Chem 7:335– 342. http://dx.doi.org/10.1002/aoc.590070507.

87. Karlson, U., & Frankenberger Jr, W. T. (1990). Volatilization of selenium from agricultural evaporation pond sediments. *Science of the total environment*, *92*, 41-54.

88. Challenger, F. (1945). Biological methylation. *Chemical Reviews*, *36*(3), 315-361.

89. Reamer, D. C., & Zoller, W. H. (1980). Selenium biomethylation products from soil and sewage sludge. *Science*, *208*(4443), 500-502.

90. Chasteen, T. G. (1993). Confusion between dimethyl selenenyl sulfide and dimethyl selenone released by bacteria. *Applied organometallic chemistry*, *7*(5), 335-342.

91. Doran JW. 1982. Microorganisms and the biological cycling of selenium, p 1–32. In Marshall KC (ed), Advances in microbial ecology. Springer, New York, NY.

92. Stork, A., Jury, W. A., & Frankenberger, W. T. (1999). Accelerated volatilization rates of selenium from different soils. *Biological trace element research*, *69*, 217-234.

93. Ranjard, L., Prigent-Combaret, C., Nazaret, S., & Cournoyer, B. (2002). Methylation of inorganic and organic selenium by the bacterial thiopurine methyltransferase. *Journal of bacteriology*, *184*(11), 3146-3149.

94. Ranjard, L., Nazaret, S., & Cournoyer, B. (2003). Freshwater bacteria can methylate selenium through the thiopurine methyltransferase pathway. *Applied and environmental microbiology*, *69*(7), 3784-3790.

95. Ranjard, L., Prigent-Combaret, C., Favre-Bonté, S., Monnez, C., Nazaret, S., & Cournoyer, B. (2004). Characterization of a novel selenium methyltransferase from freshwater bacteria showing strong similarities with the calicheamicin methyltransferase. *Biochimica et*

Biophysica Acta (BBA)-Gene Structure and Expression, *1679*(1), 80-85.

96. Chiang, P. K., Gordon, R. K., Tal, J., Zeng, G. C., Doctor, B. P., Pardhasaradhi, K., & McCann, P. P. (1996). S-Adenosylmetliionine and methylation. *The FASEB journal*, *10*(4), 471-480.

97. Levit, M. N., Liu, Y., & Stock, J. B. (1998). Stimulus response coupling in bacterial chemotaxis: receptor dimers in signaling arrays. *Molecular Microbiology*, *30*(3), 459466.

98. Reisenauer, A., Kahng, L. S., McCollum, S., & Shapiro, L. (1999). Bacterial DNA methylation: a cell cycle regulator?. *Journal of bacteriology*, *181*(17), 5135-5139.

99. van der Woude, M., Braaten, B., & Low, D. (1996). Epigenetic phase variation of the pap operon in *Escherichia coli*. *Trends in microbiology*, *4*(1), 5-9.

100. Cohen, G. N., & Cohen, G. N. (2014). The Aspartic Acid Family of Amino Acids: Biosynthesis. *Microbial Biochemistry*, 289-308.

101. Willey, J. M., Sherwood, L. M., & Woolverton, C. J. (2014). *Prescott's microbiology*. McGraw-Hill.

102. Jones DT, Taylor WR, Thornton JM (1992) The rapid generation of mutation data matricies from protein sequences. Comput Appl Biosci 8:275–282.

103. Kumar S, Stecher G, Tamura K (2016) MEGA7: Molecular Evolutionary Genetics Analysis Version 7.0 for Bigger Datasets. Mol Biol Evol 33:1870–1874. doi: 10.1093/molbev/msw054

104. Felsenstein **J** (1985) Confidence limits on phylogenies: an approach using the bootstrap. Evolution (N Y) 39:783–791. doi: 10.2307/2408678

105. Lenz, M., Smit, M., Binder, P., van Aelst, A. C., & Lens, P. N. (2008). Biological alkylation and colloid formation of selenium in methanogenic UASB reactors. *Journal of environmental quality*, *37*(5), 1691-1700.